SPCA1 governs the stability of TMEM165 in Hailey-Hailey disease

Anne-Sophie Roy, Snaigune Miskinyte, Anne Garat, Alain Hovnanian, Marie-Ange Krzewinski-Recchi, Francois Foulquier

SPCA1 governs the stability of TMEM165 in Hailey-Hailey disease

Anne-Sophie Roy[1], Snaigune Miskinyte[2,3], Anne Garat[4], Alain Hovnanian[2,3,5], Marie-Ange Krzewinski-recchi[1*], François Foulquier[1*±]

[1] Univ. Lille, CNRS, UMR 8576 – UGSF - Unité de Glycobiologie Structurale et Fonctionnelle, F- 59000 Lille, France ; [2] Laboratory of Genetic Skin Diseases, INSERM UMR1163 Imagine Institute, Paris, France ; [3] University Paris Descartes - Sorbonne Paris Cité, Paris, France ; [4] Univ. Lille, CHU Lille, Institut Pasteur de Lille, EA 4483 – IMPECS – IMPact de l'Environnement Chimique sur la Santé humaine, F-59000 Lille, France ; [5] Department of Genetics, Necker-Enfants Malades Hospital, Assistance Publique-Hôpitaux de Paris, France

* These authors contributed equally to this work

± Address correspondence should be sent to: François Foulquier, PhD, CNRS Research Director, Univ. Lille, CNRS, UMR 8576 – UGSF - Unité de Glycobiologie Structurale et Fonctionnelle, F-59000 Lille, France ; Email : francois.foulquier@univ-lille.fr; Telephone: + 33 3 20 43 44 30

Abstract

TMEM165 is a Golgi protein whose deficiency causes a Congenital Disorder of Glycosylation (CDG). We have demonstrated that Mn^{2+} supplementation could suppress the glycosylation defects observed in TMEM165-deficient cells and that TMEM165 was a Mn^{2+}-sensitive protein. In the Golgi, the other transmembrane protein capable to regulate Mn^{2+}/Ca^{2+} homeostasis is SPCA1, encoded by the *ATP2C1* gene. A loss of one copy of the *ATP2C1* gene leads to Hailey-Hailey Disease (HHD), an acantholytic skin disorder in Humans. Our latest results suggest an unexpected functional link between SPCA1 and TMEM165. In order to clarify this link in case of partial SPCA1 deficiency, HHD fibroblasts were used to assess TMEM165 expression, subcellular localization and Mn^{2+}-induced degradation. No differences were observed regarding TMEM165 expression and localization in HHD patients' fibroblasts compared to control fibroblasts. Nevertheless, we demonstrated both for fibroblasts and keratinocytes that TMEM165 expression is more sensitive to $MnCl_2$ exposure in HHD cells than in control cells. We linked, using ICP-MS and GPP130 as a Golgi Mn^{2+} sensor, this higher Mn^{2+}-induced sensitivity to a cytosolic Mn accumulation in $MnCl_2$ supplemented HHD fibroblasts. Altogether, these results link the function of SPCA1 to the stability of TMEM165 in a pathological context of Hailey-Hailey disease.

Keywords: SPCA1, Hailey-Hailey disease, TMEM165, Manganese sensitivity, Golgi

1. Introduction

SPCA1 is a Golgi protein belonging to the P-type ATPase family [1], well known to transport Ca^{2+} and Mn^{2+} from cytosol to the Golgi lumen, by hydrolyzing one ATP molecule [2,3]. The amino acids that are involved in Ca^{2+}/Mn^{2+} binding are located on M4, M5, and M6 (together with M8) transmembrane domains [4,5]. SPCA1 is known to be organized in several domains: an actuator domain (A), a phosphorylation domain (P), a nucleotide-binding domain (N or ATP binding), 5 stalk helices in the cytoplasm (S), 5 others in the intra-luminal Golgi (I) and 10 transmembrane domains [4]. This protein is highly expressed in human skin keratinocytes, and at various levels in other human tissues including skeletal muscles, kidney and mammary glands [6,7]. SPCA1 is encoded by *ATP2C1* gene, whose heterozygous loss-of-function mutations lead to a severe skin pathology named Hailey-Hailey disease (HHD) [8]. HHD is an autosomal dominant disorder characterized by painful erosions and fissures at sites of friction (neck, axillae, groin, perineum) [9]. Histologically, the main feature of this disease is a loss of adhesion between keratinocytes (acantholysis) in all suprabasal layers of the epidermis, due to a disruption of desmosomes formation [10,11]. However, to date, the acantholysis mechanisms are not completely deciphered.

Interestingly, our team recently demonstrated a functional link between SPCA1 and another Golgi protein named TMEM165 [12]. TMEM165 belongs to an uncharacterized family of transmembrane proteins, named UPF0016 (Uncharacterized Protein Family 0016) and possesses 7 transmembrane domains. *TMEM165* deficiency causes an autosomal recessive pathology, named CDG-II (*Congenital Disorder of Glycosylation),* associated with hypogalactosylation and hyposialylation of N-glycans [13–15].

The clinical phenotype of these patients is characterized by a severe psychomotor retardation, a major skeletal dysplasia leading to a dwarfism and an osteoporosis [13]. We have interestingly shown that TMEM165–associated glycosylation defects could be restored by $MnCl_2$ supplementation in the culture medium. Although its function remains unclear, our team previously demonstrated that TMEM165 was a highly manganese sensitive protein. Indeed, when cells are exposed to supraphysiological $MnCl_2$ concentrations (500µM of $MnCl_2$ for 8h), TMEM165 was shown to be targeted to and degraded in lysosomes [16]. Altogether, these results suggest that TMEM165 could play a role as a Mn^{2+} transporter, in Golgi Mn^{2+} homeostasis.

By using KO SPCA1 cells, we recently highlighted that TMEM165 expression was dependent on SPCA1 capacity to import Mn^{2+} into the Golgi lumen [12]. In Hailey-Hailey disease patients' cells, SPCA1 is partially deficient due to a loss of one functional copy of *ATP2C1* gene. Therefore, in order to explore the potential link between TMEM165 and SPCA1 in

Hailey-Hailey disease, we investigated whether partial deficiency of SPCA1 had an impact on TMEM165 expression, localization and Mn^{2+}-induced degradation. In this paper, we demonstrated that TMEM165 degradation in fibroblasts and keratinocytes from all studied HHD patients is more sensitive to increased extracellular $MnCl_2$ concentrations than normal human fibroblasts (NHF) and/or keratinocytes (NHK). This links the functionality of SPCA1 to the stability of TMEM165 in HHD fibroblasts/keratinocytes under $MnCl_2$ exposure. Altogether, our results suggest that the Mn^{2+}-induced TMEM165 degradation sensitivity can be used as a sensor assay to monitor the functionality of SPCA1 in Hailey-Hailey disease patients' cells.

2. Material and methods

2.1. Antibodies and other reagents

Anti-TMEM165 and β-actin antibodies were purchased from Sigma-Aldrich (Saint Louis, OM, USA). Anti-SPCA1 antibodies were purchased from Santa Cruz (California) used in immunofluorescence staining (IF), Abcam (Cambridge, United Kingdom) used in proximity ligation assay (PLA), and Abnova (Taiwan) used in western-blotting (WB). Anti-GM130 antibody was purchased from BD Biosciences (Franklin Lakes, NJ, USA), anti-LAMP2 from Santa Cruz and anti-GPP130 from Biolegend (San Diego, California). Alexa Fluor 488-Giantin antibody was purchased from Biolegend and used in PLA. Polyclonal goat anti-rabbit or anti-mouse immunoglobulins HRP conjugated were purchased from Dako (Glostrup, Denmark). Polyclonal goat anti-rabbit or anti-mouse conjugated with Alexa Fluor was purchased from Thermo Fisher Scientific (Waltham, MA, USA). Manganese (II) chloride tetrahydrate was provided from Riedel-deHaën (Seelze, Germany) and chloroquine from ICN biomedicals inc. (Ohio).

2.2.Cell culture

2.2.1. HHD patient selection

Normal human (NHF and NHK) and HHD fibroblasts and keratinocytes were provided by Pr. Alain HOVNANIAN and in part studied in IMAGINE institute. These cells were obtained from normal skin from punch biopsies, after patient consent. All patients studied were diagnosed with HHD before entry into the study, demonstrating typical clinical findings (blistering and erosion in characteristic locations) and histopathologic pathology (acantholysis of suprabasal cells without apoptosis). All patients signed consent forms in accordance with the local ethics committee protocol. Table 1 indicates the mutations of the *ATP2C1* gene occurring in HHD

fibroblasts (A) and keratinocytes (B) cells used in this study. The HHD 1 patient carried on intron 22 of the *ATP2C1* gene that can affect the M5 transmembrane domain. The HHD 2 and 3 patients shared an already known missense mutation I580V belonging to the ATP-binding domain [4]. One other missense mutation M359K in M5 domain is described for HHD 5 patient. The other HHD patients, HHD 4 and 6 carried mutations which generating truncated protein with premature termination codon respectively in the actuator and M7 domains. Missense mutations or PTC (premature termination codon) could affect the stability, the subcellular localization or the functionality of SPCA1. Mutations carried on *ATP2C1* gene, for HHD 1, HHD 4 and HHD 5 patients are new mutations not yet been reported.

In this study, fibroblasts cells were used for the patients HHD 1, HHD 2, HHD 3 and HHD 4, and keratinocytes cells for the patients HHD 2, HHD 5, HHD 6.

Normal human keratinocytes (NHK) and fibroblasts (NHF) matched to, sex, location skin biopsy, and pass number were used as controls.

2.2.2. Fibroblasts culture

Normal human (NHF) and HHD fibroblasts were maintained in Dulbecco's modified Eagle's Medium (DMEM; Lonza, Basel, Switzerland) supplemented with 10% fetal bovine serum (FBS; Corning, USA), at 37°C in humidity-saturated 5% CO_2 atmosphere.

2.2.3. Keratinocytes culture

Cells were maintained in Green medium on a feeder layer of lethally irradiated 3T3 mouse fibroblasts as described previously [17], at 37°C in humidity-saturated 10% CO_2 atmosphere. For WB assay, cells were grown in 0.06 mM Ca^{2+} Epilife medium (Invitrogen, Waltham, MA) and collected after treatment with $MnCl_2$. For keratinocytes differentiation, cells were grown in 1.2 mM Ca^{2+} Epilife medium for 7 days.

2.3.Western-blotting

After treatment, cells were pelleted and resuspended in RIPA buffer [Tris/HCl (pH 7.6) 25mM, NaCl 150mM, Triton X-100 1%, Sodium deoxycholate 1%, SDS 0.1%] with a cocktail of protease inhibitors (Roche Diagnostics, Penzberg, Germany). Then, cells were lysed in an ultrasonic bath (Bioblock Scientific) for 2 minutes and centrifuged for 30 min at 20 000xg at 4°C. The protein concentration of extracted proteins was determined with the Micro BCA Protein Assay kit (Thermo Scientific). 10µg of total protein lysate was dissolved in Laemly buffer 1X [Laemly buffer 5X: Tris/HCl (pH 6.8) 60mM, glycerol 50%, SDS 2%, Bromophenol

blue 1%] supplemented with 4% β-mercaptoethanol (Sigma-Aldrich). Each sample was separated by SDS-PAGE on 10% acrylamide gels (Invitrogen) and transferred to a nitrocellulose membrane with i-blot 2 Dry Blotting System (Thermo Fisher Scientific). The membranes were incubated in blocking buffer [5% milk (β-actin and β-tubulin antibodies) or BSA (SPCA1 and TMEM165 antibodies) powder in TBST (1X TBS [euromedex] with 0.05% Tween 20 [euromedex]) overnight at 4°C and, then, incubated 1h at room temperature with primary antibodies (diluted at 1/20000 for β-actin, 1/10000 for β-tubulin, 1/3000 for TMEM165 and 1/4000 for SPCA1) in blocking buffer. After three washes for 5 min with TBST, the membranes were incubated with the peroxidase-conjugated secondary goat anti-rabbit (Dako; used at the dilution of 1/10000) or goat anti-mouse (Dako; used at the dilution of 1/20000) antibodies in blocking buffer for 1h at room temperature and afterward washed 3 times for 5 min with TBST. Signal was detected with chemiluminescence reagent (SuperSignal^{TM} West Pico PLUS Chemiluminescent Substrate, Thermo Fisher Scientific) on camera (fusion, Vilber).

2.4. Immunofluorescence

Cells were seeded on coverslips for 24h and subjected to the indicated treatments, washed twice in Dulbecco's Phosphate Buffer Saline (DPBS$^{+/+}$, Lonza) and fixed with 4% paraformaldehyde (PFA) in PBS 1X (pH 7.4), for 20 min at room temperature. Coverslips were then washed three times with PBS 1X and were put in a humidity chamber. Cells were permeabilized with 0.5% Triton X-100 in PBS 1X for 10 min then washed three times with PBS 1X. Coverslips were saturated for 1h in BSA-Block (Candor-bioscience, Germany) and then in incubation for 2h with primary antibody diluted either at 1/100 (anti-SPCA1 and anti-GPP130), or 1/300 (anti-TMEM165, anti-GM130 and anti-LAMP2) in BSA-block. After washing with PBS 1X, cells were incubated 1h with Alexa 488- or Alexa 568-conjugated secondary antibody (Life Technologies or Invitrogen) diluted at 1/600 in BSA-block. After washing with PBS 1X, coverslips were mounted on glass slides with Mowiol. Fluorescence was detected through an inverted Zeiss LSM700 confocal microscope.

2.5. Proximity Ligation Assay (PLA) and microscopy analysis

PLA was performed using the Duolink® PLA Kit (Sigma-Aldrich) with red detection reagents (DUO92008), anti-mouse MINUS probe (DUO92004) and anti-rabbit PLUS probe (DUO92002). Cells were fixed, blocked and incubated with primary antibodies as for standard IF (see IF section). After two washes with buffer A 1X, anti-mouse MINUS and anti-rabbit

PLUS were added (diluted 1:5 in Antibody diluent) on coverslips and incubated in a humidity chamber (60 minutes, at 37°C). Ligation (30 minutes, at 37°C) and amplification (120 minutes, at 37°C) steps were performed using Detection Duolink Kit according to the manufacturer's protocol. To analyse the localization of PLA red spots, Alexa Fluor 488-Giantin was used before the last two washes with buffer B 1X and with buffer B 0.01X. Coverslips were then mounted on glass slides with Mounting Medium including DAPI (DUO82040). Images were taken on a Zeiss LSM700 confocal microscope. PLA was quantified as the number of spots divided by the nuclei number of cells. All analysis was performed by TisGolgi.

2.6. Image analyses

Acquisitions and quantification were done using TisGolgi, a home-made ImageJ (http://imagej.nih.gov/ij) plugin developed by TISBio and available upon request. This program detects and quantifies the intensity of associated Golgi and vesicles fluorescence, based on morphological parameters such as size and circularity. And then, this program calculates for each image the number of detected signals and the mean of fluorescence intensity. The microscope settings were kept constant for all images to enable direct comparison. The quantification was performed on one set of experiments when all stainings were performed at the same time. The threshold used for the quantification was constant in a set of experiments.

2.7. ICP-MS (Inductively Coupled Plasma-Mass Spectrometry)

2.7.1. Sample preparation

After manganese treatment in T25 flasks, cells were washed twice with PBS 1X on ice, then resuspended in 1mL of PBS 1X: 200µL were kept to protein dosage and 800µL for manganese (Mn) measurement by ICP-MS. Both were centrifuged for 10 min at 10 000xg at 4°C. Afterward, cellular pellets for protein dosage were resuspended and lysed with RIPA buffer as indicated in the western-blot section. Protein concentration was determined by the Micro BCA Protein Assay kit (Thermo Scientific). Cellular pellets for Mn measurement were resuspended with 100µL of deionized water and sonicated 1 min. A methanol/chloroform/sample extraction was done (ratio 1:2:3). The upper phase containing soluble material was kept and dried with a concentrator for 1h30 at 45°C (concentrator 5301, Eppendorf). Finally, samples were dissolved with 200µL of deionized water.

2.7.2. Mn measurement and analysis

Samples were diluted 50 times with 1.5% (v/v) nitric acid (ultrapure quality 69.5%, Carlo Erba Reagents, Val de Reuil, France) solution in ultrapure water (Purelab Option-Q, Veolia Water, Antony, France) containing 0.1% TritonX-100 (Euromedex, Souffelweyersheim, France), 0.2% butan-1-ol (VWR chemicals, Fontenay-sous-Bois, France), and 0.5µg/L rhodium (Merck, Darmstadt, Germany). The analysis was performed on an ICP-MS THERMO ICAP^{TM} Q (Thermo Scientific, Courtaboeuf Cedex, France). The limit of quantification was 0.2µg/L.

2.8. Statistical analysis

Comparisons between groups were performed using Student's t-test for two variables with different or equal variances depending on the result of the F-test. Relative EC50 was calculated by https://www.aatbio.com/tools/ec50-calculator.

3. Results

3.1. Expression and localization of TMEM165 and SPCA1 in Hailey-Hailey disease patients' cells

In order to explore whether heterozygous loss-of-function mutations in the *ATP2C1* gene in HHD patients' cells could impact the functional link between TMEM165 and SPCA1, their expression levels were first assessed by western-blot experiments (**Fig. 1A**). Fibroblasts from 4 Hailey-Hailey disease patients (HHD 1 to 4) and two control human fibroblasts (NHF 1 and 2) were first used. Using anti-SPCA1 antibody, whose detection specificity was previously assessed [12], a major band at 100 kDa, corresponding to the molecular weight of SPCA1, was detected in all HHD and control fibroblasts (**Fig. 1A**). The use of anti-TMEM165 antibody as previously reported, led to the detection of two major bands around 35 kDa [15]. While TMEM165 expression was not significantly affected, SPCA1 expression was found lower in HHD fibroblasts compared to controls (**Fig. 1A**). The quantification highlights that the relative expression of SPCA1 was between 40 to 66% in HHD fibroblasts, compared to control human fibroblasts NHF 1 and NHF 2 (**Fig. 1B**).

We next investigated by immunofluorescence, the subcellular localization of TMEM165 and SPCA1 (**Fig. 1C and D**). First, co-localization experiments with the Golgi marker GM130 confirmed the subcellular Golgi localization of TMEM165 in all investigated fibroblasts (**Fig. 1C**). Hence the *ATP2C1* gene mutations have no obvious impacts on subcellular Golgi TMEM165 localization. Next and as expected, the subcellular localization of SPCA1 was found co-localized with TMEM165 in all fibroblasts (**Fig. 1D**) then arguing for its correct Golgi localization. In agreement with the obtained western-blot results, the quantification of the mean fluorescence intensity of SPCA1 showed a pronounced decrease in all HHD patient fibroblasts compared to controls (**Fig. 1E**). The TMEM165 associated fluorescence intensity is found similar between patient and control cells (**Fig. 1E**). Altogether these results demonstrate that the partial lack of SPCA1 in HHD fibroblasts does not affect the expression/ subcellular localization of TMEM165, but only affects the steady state expression level of SPCA1.

3.2. TMEM165 and SPCA1 proximity in HHD patients' cells

According to our recent results in Hap1 cells, a proximity between TMEM165 and SPCA1 was shown [12]. Although the subcellular localization of these two proteins is not affected, it could well be that SPCA1 mutations could prevent the proximity with TMEM165. To tackle this question, we then investigated *in situ* associations of TMEM165 and SPCA1 in control and

HHD patients' fibroblasts using proximity ligation assay (PLA). Theoretically, each PLA dot is the result of the close proximity of one molecule of SPCA1 and one molecule of TMEM165. As observed in **Figure 2A**, we obtained PLA red positive signals in all investigated control and patient fibroblasts. To demonstrate the specificity of the detection, two negative controls were used. In the first control experiment, one of the primary antibodies was omitted and in the second control experiment, fibroblasts were prior incubated with 500µM $MnCl_2$ in order to completely destabilize TMEM165 (**Fig. 2B and Fig. 3A**). As expected, no signal was detected in these two negative control experiments then demonstrating the specificity of the detection and hence the *in situ* proximity of SPCA1 and TMEM165 proteins. We then quantified the number of PLA positive signals per cell (**Fig. 2C**). A lower number of PLA signals per nucleus in HHD fibroblasts (20 to 27) compared to NHFs (42 to 44) was observed. As PLA signal is depending on protein expression levels, we then quantified PLA events by taking into account the observed difference in SPCA1 expression level between controls and HHD patients' cells. In this refined quantification (**Fig. 2D**), no obvious differences between control (0.98 to 1.1) and HHD patients' fibroblasts (0.82 to 1.16) were observed. To then assess the subcellular localization of the PLA signal, Giantin-alexa fluor 488 antibody was used in PLA experiment. A clear overlap of Giantin and PLA signals, confirming the Golgi localization of the proximity between TMEM165 and SPCA1 was seen (**Fig. 2E**). These results clearly highlight the close proximity of SPCA1 and TMEM165 in HHD patients' fibroblasts and also suggest that the expression of a mutated SPCA1 form does not seem to affect its interaction with TMEM165.

3.3. Impact of manganese exposure on TMEM165 expression in HHD versus control cells

According to our previous works [16], TMEM165 rapidly degrades into lysosomes under supraphysiological $MnCl_2$ supplementation. We then wondered whether $MnCl_2$ supplementation could differentially affect TMEM165 expression in SPCA1-deficient fibroblasts compared to controls. In order to address this question, we treated control and HHD fibroblasts with increasing $MnCl_2$ concentrations (0 to 500µM) for 8h (**Fig. 3**). No cell death was observed with these $MnCl_2$ concentrations. TMEM165 expression was first analyzed by western-blot. In both cell types, TMEM165 rapidly disappears followed $MnCl_2$ supplementation (**Fig. 3A**) but we can observe that its sensitivity however significantly differs. While 300µM $MnCl_2$ was required to induce TMEM165 destabilization in control cells (NHF 1 and NHF 2), our results show that only 50-100µM of $MnCl_2$ was sufficient to induce a destabilization in HHD patients' fibroblasts. Quantification indicated that TMEM165 loss

exceeded 90% after 8h of treatment with 50µM $MnCl_2$ in HHD fibroblasts while only 60-72% decrease was seen in control cells (**Fig. 3B**).

This observation was confirmed by immunofluorescence staining followed by confocal microscopy where a decrease in Golgi-associated TMEM165 fluorescence intensity was also seen according to the increasing $MnCl_2$ concentrations (**Fig. S1A**). It is to note that in all investigated conditions, there was no change in SPCA1 fluorescence intensity and Golgi localization. The quantification of the TMEM165 Golgi associated fluorescence confirmed the higher Mn^{2+} sensitivity of TMEM165 in HHD patients' cells compared to controls (**Fig. S1B**). Interestingly, two different groups of HHD patients emerge from this quantification. While TMEM165 expression after 50µM of $MnCl_2$ for 8h exposure ranged between 88-92% in control cells, the expression was between 65-69% for the group HHD 1/HHD 4 and 0-5% for the group HHD 2/HHD 3 patient cells (**Fig. S1B**). To tweak this result, TMEM165 expression was followed by immunofluorescence using lower $MnCl_2$ concentrations (1 and 10µM for 8h) (data not shown). TMEM165 quantification led us to calculate the relative EC50 of $MnCl_2$ for each patient and control cells. The obtained results (**Fig. S2**) confirmed the presence of two groups of patients distinct in their TMEM165 Mn^{2+} sensitivity. While the relative EC50 after 8h of $MnCl_2$ exposure on TMEM165 expression indeed ranged around 137µM of $MnCl_2$ for control cells, an EC50 of 17µM $MnCl_2$ was calculated for HHD 2 and HHD 3 (same missense I580V mutation) patient cells, and 56µM $MnCl_2$ for HHD 1 and HHD 4 patient cells (**Fig. S2**). Altogether these results demonstrate a functional link between SPCA1 and TMEM165 in HHD patients' fibroblasts under $MnCl_2$ supplementation.

3.4.Effect of chloroquine on the Mn^{2+}-induced decrease of TMEM165 in HHD patients' cells

In order to confirm that the observed decrease of TMEM165 expression upon $MnCl_2$ exposure corresponded to lysosomal degradation, we performed western-blot (**Fig. 4**) and immunofluorescence experiments (**Fig. S3**) in presence of chloroquine, a weak base raising the pH of acidic compartments. This was assayed using 100µM of chloroquine in control fibroblasts treated with 500µM of $MnCl_2$ and HHD fibroblasts treated with 100µM of $MnCl_2$ (two concentrations where none expression of TMEM165 could be detected).

As expected, control and HHD fibroblasts treated with $MnCl_2$ showed a dramatic loss of TMEM165 expression (**Fig. 4A**). In contrast, the abundance of TMEM165 was recovered in all $MnCl_2$/ chloroquine treated cells (**Fig. 4A**). Quantification indicated an average of 60% rescue of TMEM165 levels in HHD cells treated with both $MnCl_2$ and chloroquine (**Fig. 4B**).

Immunofluorescence experiments and co-localization studies with LAMP2, a lysosomal marker, showed the presence of TMEM165 in LAMP2-positive structures in both chloroquine- and $MnCl_2$-treated cells (**Fig. S3**), then demonstrating the lysosomal degradation of TMEM165 induced by $MnCl_2$ exposure. These results are in accordance with all our previous findings demonstrating that the observed Mn^{2+} induced loss of expression of TMEM165 results from its targeting and degradation in lysosomes.

3.5. Quantification by ICP-MS of the intracellular Mn level in HHD and control cells cultured in absence and in presence of $MnCl_2$

Our previous study using isogenic Hap1 KO SPCA1 cells showed that TMEM165 abundance was directly dependent on SPCA1's function and more specifically its capacity to pump Mn^{2+} from the cytosol into the Golgi lumen [12]. The cytosolic Mn^{2+} accumulation resulting from a complete lack of SPCA1 functionality, triggers the Mn^{2+} induced lysosomal degradation of TMEM165. The observed differential Mn^{2+} TMEM165 sensitivity between control and HHD fibroblasts led us to investigate the intracellular Mn levels in control and HHD fibroblasts. To do this, ICP-MS *Inductively Coupled Plasma-Mass Spectrometry*) experiments were first performed in control and HHD fibroblasts cultured in presence and in absence of 5µM $MnCl_2$ supplementation (**Fig. 5**). This concentration does not affect the stability of TMEM165 and allows us to study SPCA1 functionality. Indeed, as shown in **figure S4**, no TMEM165 destabilization is observed in control and HHD patients' fibroblasts when cells are cultured in presence of 5µM $MnCl_2$. Without $MnCl_2$ supplementation, the Mn steady state level was found similar between control and HHD fibroblasts (Fig.5A). The cells were next incubated with 5µM $MnCl_2$ for 1h and 2h prior ICP-MS analysis. While the intracellular Mn level measured by ICP-MS shows an average of 1.8-fold increase in control cells, an average of 3.1-fold increase is interestingly observed in HHD fibroblasts (**Fig. 5B**). These results highly suggest that the partial lack of SPCA1 in HHD fibroblasts leads to a higher Mn accumulation compared to control cells followed $MnCl_2$ supplementation.

To determine whether this higher Mn accumulation in HHD fibroblasts could be cytosolic, control and HHD fibroblasts were treated with 500µM $MnCl_2$ for 0, 8h, 12h and 24h and the stability of GPP130, a Golgi Mn^{2+} sensor [18,19] was tested by immunofluorescence. A significant difference in GPP130 fluorescence intensity was observed between control and HHD fibroblasts after $MnCl_2$ treatment (**Figure S5**). While in control cells the associated GPP130 fluorescence intensity decreases under $MnCl_2$ treatment (~80% after 24h of $MnCl_2$

incubation), its remains stable in HHD fibroblasts. The quantification of the mean fluorescence intensity of GPP130 under $MnCl_2$ treatment was shown in **figure 6**. As GPP130 is found less sensitive to $MnCl_2$ exposure in HHD fibroblasts compared to control fibroblasts, it is likely that the observed increase Mn in HHD fibroblasts is cytosolic.

3.6. Impact of manganese exposure on TMEM165 expression in HHD versus control keratinocytes

As keratinocytes represent the major population of epidermal cells, they constitute a model for investigating the pathological features of Hailey-Hailey disease. The Mn^{2+}-induced TMEM165 sensitivity was then investigated in keratinocytes from HHD patients cultured in presence or in absence of 50µM $MnCl_2$ for 48h differentiated or not with 1.2mM $CaCl_2$ during 7 days (**Fig. 7**). All HHD patients' keratinocytes showed a lower SPCA1 expression compared to normal human keratinocytes (NHKs) (data not shown).

In undifferentiated keratinocytes, no major significant differences in TMEM165 expression were observed between HHD and NHKs, except for HHD 5, in which a slight decrease in TMEM165 expression could be observed. After 50µM $MnCl_2$ exposure on undifferentiated keratinocytes (**Fig. 7A**), the remaining TMEM165 expression was 8% for HHD 5 and 58-71% for HHD 6/ HHD 2, compared to 98-104% for NHK 1/ NHK 2. The result is however strikingly different on differentiated keratinocytes where TMEM165 expression ranged from 2% to 28% in HHD patients compared to 80-92% in control keratinocytes followed $MnCl_2$ exposure (**Fig. 7B**). The observed Mn^{2+}-induced decrease of TMEM165 expression appears more pronounced in differentiated compared to undifferentiated keratinocytes (**Fig. 7C**). This is particularly the case for HHD 2 and HHD 6 patients where 50µM $MnCl_2$, 48h exposure induced a stronger decrease of TMEM165 expression in differentiated keratinocytes compared to undifferentiated keratinocytes. In conclusion, the Mn^{2+} induced decrease of TMEM165 is observed in HHD keratinocytes in the same way as HHD fibroblasts.

4. Discussion

SPCA1 is known as the main Golgi P-Type Ca^{2+}/Mn^{2+} pump regulating Ca^{2+}/Mn^{2+} concentrations at the Trans Golgi Network [20]. Mutations in the *ATP2C1* gene encoding SPCA1 lead to a rare autosomal dominant disease called Hailey-Hailey disease (HHD) [3]. The main features are severe skin damages with blistering. The pathogenesis is not fully understood but results from a defect in keratinocytes differentiation linked due to the deregulation of the keratinocyte cytosolic Ca^{2+} concentration and leading to the abnormal processing of desmosomal proteins [21,22]. The consequence is a defect in epidermal integrity resulting from a lack of keratinocytes adherence called acantholysis. Our previous works suggested that beside the fundamental role of SPCA1 in regulating Golgi Ca^{2+}/ Mn^{2+} homeostasis, TMEM165 would be another key actor in Golgi Ca^{2+}/Mn^{2+} homeostasis. TMEM165 has been related to inherited disorders in humans called CDG for Congenital Disorders of Glycosylation [13] where TMEM165 defects are associated to strong Golgi glycosylation abnormalities [15]. Although clinical phenotypes are completely different from those observed in Hailey-Hailey disease, our previous works in yeasts suggested a link between Gdt1 and Pmr1, the yeast orthologs of TMEM165 and SPCA1 respectively [23]. Moreover, we recently investigated this link in mammalian cell lines using isogenic SPCA1 KO Hap1 cells and we demonstrated that the steady state level of TMEM165 was depending on SPCA1's function and more specifically its ability to import Mn^{2+} inside the Golgi lumen [12].

To summarize the concept, a complete loss of TMEM165 was observed when SPCA1 was absent and we demonstrated that only the Q747A SPCA1 mutant that favors Mn^{2+} pumping rescues the abundance and subcellular Golgi localization of TMEM165. In this model, the lack of SPCA1 functionality leads to a dramatic Mn^{2+} cytosolic increase that destabilizes TMEM165. But what happens in case of partial SPCA1 deficiency?

To tackle this point, we took advantage in this study of the Hailey-Hailey disease caused by the loss of one copy of the *ATP2C1* gene. By using both fibroblasts and keratinocytes cultured from patients with Hailey-Hailey disease, TMEM165 expression level, subcellular localization and Mn^{2+} sensitivity were scrutinized. As observed in other studies, mutations in *ATP2C1* gene reduce the cellular amount of SPCA1 [22,24]. Approximately half of the protein is seen compared to controls. For two of the studied patients (HHD 4 and 6), the SPCA1 mutations generate a truncated protein undetected by western-blot as likely unstable and prone to degradation. For the two other patients HHD 2 and HHD 3, carrying the same I580V missense

mutation, the impact of this mutation on protein functionality is not clear as it has been previously demonstrated that this mutation does not really prevent the Ca^{2+} and Mn^{2+} transport when expressed in a Δ*PMR1* yeast background [25]. Moreover, Fairclough et al. demonstrated that the I580V mutation could disrupt the crucial conformational change allowing the transport of Mn^{2+} or Ca^{2+} in the Golgi lumen [26]. In our hands the stability of SPCA1 is affected in those patients carrying the I580V missense mutation probably reflecting different degrees of SPCA1 impairment among different patients, as it has been seen in studies to correlate molecular and clinical results in HHD patients [27]. One can maybe expect that this mutation acts as a dominant negative on wt-SPCA1 form leading to the degradation of half of SPCA1. Altogether, these results support the fact that haploinsufficiency is certainly the prevalent mechanism for the dominant inheritance of HHD [28]. Although the amount of SPCA1 is decreased, the steady state level of TMEM165 in HHD patients was found unchanged and comparable to the one observed in control cells. As such this result suggests that the functionality of half of SPCA1 protein is sufficient to prevent the cytosolic Mn^{2+} accumulation that would engage TMEM165 in the lysosomal targeting and degradation way. This result is moreover reinforced by the fact that the measure of the steady state Mn level by ICP-MS, in absence of Mn supplementation, is similar in HHD patient and control cells.

We then assessed the Mn^{2+} sensitivity of TMEM165 in HHD patients. We interestingly showed that the sensitivity of TMEM165 to $MnCl_2$ exposure was higher for HHD patients compared to control cells. While in control fibroblasts TMEM165 expression is sensitive to 300µM, 8h of $MnCl_2$ exposure, TMEM165 expression completely disappears in HHD patient's fibroblasts followed 50µM, 8h of $MnCl_2$ exposure. As observed in other studies, the Mn^{2+} induced TMEM165 degradation mechanism results from a lysosomal degradation and is then exacerbated in HHD fibroblasts. Altogether these results reinforce a functional relationship between SPCA1 functionality and the intracellular steady state level of TMEM165.

The underlying mechanism is based on the impact of a lack of SPCA1 functionality on the cytosolic Mn^{2+} accumulation after $MnCl_2$ exposure. This has been confirmed by ICP-MS where an increased accumulation of Mn is observed in HHD fibroblasts after $MnCl_2$ exposure compared to control cells. The use of GPP130 as a sensor of Golgi Mn^{2+} homeostasis confirmed the cytocolic Mn accumulation in HHD fibroblasts compared to control fibroblasts under $MnCl_2$ supplementation. Altogether, these results demonstrate that the partial SPCA1 deficiency in HHD makes these cells more sensitive to $MnCl_2$ exposure and likely results in a higher cytosolic Mn^{2+} accumulation than in control cells. As such, TMEM165 is then found more sensitive to $MnCl_2$ exposure in HHD cells.

Our results also highlight that this is not restricted to HHD fibroblasts as similar results were observed in patients' keratinocytes. The only difference lies in the differentiation state. We indeed showed that TMEM165 was more sensitive to $MnCl_2$ exposure in differentiated keratinocytes compared to undifferentiated keratinocytes. It is important to note that Ca^{2+} not only induces but also regulates keratinocytes differentiation, a fundamental process for the formation of an intact epidermal barrier [29]. Abnormally high cytoplasmic Ca^{2+}, a feature of HHD keratinocytes, alters processing of desmosomal proteins [10]. As SPCA1 is known to have the same affinity for Ca^{2+} and Mn^{2+} ions, it is likely that an accumulation of cytoplasmic Ca^{2+} in differentiated HHD keratinocytes prevents the Mn^{2+} import inside the Golgi. Under $MnCl_2$ exposure, the consequence is an increased cytosolic Mn^{2+} accumulation that leads to a destabilization of TMEM165. Although the Ca^{2+}-dependent mechanisms in desmosome assembly has been well investigated in HHD, the impact of cytosolic Mn^{2+} accumulation remains not deciphered. It could well be that environmental factors modifying extracellular Mn^{2+} environment such as diet may greatly influence the etiology of the Hailey-Hailey disease.
Interestingly no obvious glycosylation defect was observed on reporter glycoproteins such as LAMP2 and TGN46 in HHD patients' cells. This result that is consistent with our study on Hap1 KO SPCA1 cells certainly lies in the alternative pathways taken by accumulating cytosolic Mn to reach the Golgi lumen. Our previous results suggest the importance of the ER in such process [30].

5. Conclusion

At the fundamental point of view, our results link unambiguously the function of SPCA1 to the stability of TMEM165 in pathological conditions. Moreover, our results show that the follow-up of the Mn^{2+}-induced TMEM165 degradation in HHD could be used to i_ study the functionality of SPCA1 and more especially the impacts of SPCA1 mutations and ii_ evaluate the effects of any potential treatments.

Acknowledgements

We are indebted to Dr Dominique Legrand for the Research Federation FRABio (Univ. Lille, CNRS, FR 3688, FRABio, Biochimie Structurale et Fonctionnelle des Assemblages Biomoléculaires) for providing the scientific and technical environment conducive to achieving this work. We thank the BioImaging Center of Lille for the use of the Leica LSM700 and the Leica LSM780.

Authors' contribution

Conception of the work: F.F., A.H., M.A.K., Performed experiments: A.S.R., Contributed reagents/materials: S.M., A.H., Analyzis of data: A.S.R., A.G., M.A.K., Wrote the paper: F.F., A.S.R.,

Competing interests

There are no actual or perceived conflicts of interest associated with this manuscript.

Funding information

This work was supported by grants from Agence Nationale de la Recherche (SOLV-CDG project to FF), EUROGLYCAN-omics that was supported by ANR, under the frame of E-RARE-3, the ERA-Net for Research on Rare Diseases and within the scope of the International Associated Laboratory "Laboratory for the Research on Congenital Disorders of Glycosylation – from cellular mechanisms to cure – GLYCOLAB4CDG".

References

[1] P. Vangheluwe, M.R. Sepúlveda, L. Missiaen, L. Raeymaekers, F. Wuytack, J. Vanoevelen, Intracellular Ca2+- and Mn2+-transport ATPases, Chem. Rev. 109 (2009) 4733–4759. https://doi.org/10.1021/cr900013m.

[2] L. Foggia, A. Hovnanian, Calcium pump disorders of the skin, Am J Med Genet C Semin Med Genet. 131C (2004) 20–31. https://doi.org/10.1002/ajmg.c.30031.

[3] L. Missiaen, L. Raeymaekers, L. Dode, J. Vanoevelen, K. Van Baelen, J.B. Parys, G. Callewaert, H. De Smedt, S. Segaert, F. Wuytack, SPCA1 pumps and Hailey–Hailey disease, Biochemical and Biophysical Research Communications. 322 (2004) 1204–1213. https://doi.org/10.1016/j.bbrc.2004.07.128.

[4] M. Micaroni, G. Giacchetti, R. Plebani, G.G. Xiao, L. Federici, ATP2C1 gene mutations in Hailey-Hailey disease and possible roles of SPCA1 isoforms in membrane trafficking, Cell Death Dis. 7 (2016) e2259. https://doi.org/10.1038/cddis.2016.147.

[5] S. Mukhopadhyay, A.D. Linstedt, Identification of a gain-of-function mutation in a Golgi P-type ATPase that enhances Mn2+ efflux and protects against toxicity, Proc. Natl. Acad. Sci. U.S.A. 108 (2011) 858–863. https://doi.org/10.1073/pnas.1013642108.

[6] N.B. Pestov, R.I. Dmitriev, M.B. Kostina, T.V. Korneenko, M.I. Shakhparonov, N.N. Modyanov, Structural evolution and tissue-specific expression of tetrapod-specific second isoform of secretory pathway Ca2+-ATPase, Biochem. Biophys. Res. Commun. 417 (2012) 1298–1303. https://doi.org/10.1016/j.bbrc.2011.12.135.

[7] L.L. Wootton, C.C.H. Argent, M. Wheatley, F. Michelangeli, The expression, activity and localisation of the secretory pathway Ca2+ -ATPase (SPCA1) in different mammalian tissues, Biochim. Biophys. Acta. 1664 (2004) 189–197. https://doi.org/10.1016/j.bbamem.2004.05.009.
[8] R. Sudbrak, J. Brown, C. Dobson-Stone, S. Carter, J. Ramser, J. White, E. Healy, M. Dissanayake, M. Larrègue, M. Perrussel, H. Lehrach, C.S. Munro, T. Strachan, S. Burge, A. Hovnanian, A.P. Monaco, Hailey–Hailey disease is caused by mutations in ATP2C1 encoding a novel Ca2+ pump, Hum. Mol. Genet. 9 (2000) 1131–1140. https://doi.org/10.1093/hmg/9.7.1131.
[9] J. Dhitavat, R.J. Fairclough, A. Hovnanian, S.M. Burge, Calcium pumps and keratinocytes: lessons from Darier's disease and Hailey-Hailey disease, Br. J. Dermatol. 150 (2004) 821–828. https://doi.org/10.1111/j.1365-2133.2004.05904.x.
[10] M. Hakuno, H. Shimizu, M. Akiyama, M. Amagai, J.K. Wahl, M.J. Wheelock, T. Nishikawa, Dissociation of intra- and extracellular domains of desmosomal cadherins and E-cadherin in Hailey-Hailey disease and Darier's disease, Br. J. Dermatol. 142 (2000) 702–711.
[11] D. Metze, H. Hamm, A. Schorat, T. Luger, Involvement of the adherens junction-actin filament system in acantholytic dyskeratosis of Hailey-Hailey disease. A histological, ultrastructural, and histochemical study of lesional and non-lesional skin, J. Cutan. Pathol. 23 (1996) 211–222.
[12] E. Lebredonchel, M. Houdou, H.-H. Hoffmann, K. Kondratska, M.-A. Krzewinski, D. Vicogne, C.M. Rice, A. Klein, F. Foulquier, Investigating the functional link between TMEM165 and SPCA1, Biochem. J. 476 (2019) 3281–3293. https://doi.org/10.1042/BCJ20190488.
[13] F. Foulquier, M. Amyere, J. Jaeken, R. Zeevaert, E. Schollen, V. Race, R. Bammens, W. Morelle, C. Rosnoblet, D. Legrand, D. Demaegd, N. Buist, D. Cheillan, N. Guffon, P. Morsomme, W. Annaert, H.H. Freeze, E. Van Schaftingen, M. Vikkula, G. Matthijs, TMEM165 Deficiency Causes a Congenital Disorder of Glycosylation, The American Journal of Human Genetics. 91 (2012) 15–26. https://doi.org/10.1016/j.ajhg.2012.05.002.
[14] W. Morelle, S. Potelle, P. Witters, S. Wong, L. Climer, V. Lupashin, G. Matthijs, T. Gadomski, J. Jaeken, D. Cassiman, E. Morava, F. Foulquier, Galactose Supplementation in Patients With TMEM165-CDG Rescues the Glycosylation Defects, J. Clin. Endocrinol. Metab. 102 (2017) 1375–1386. https://doi.org/10.1210/jc.2016-3443.
[15] S. Potelle, W. Morelle, E. Dulary, S. Duvet, D. Vicogne, C. Spriet, M.-A. Krzewinski-Recchi, P. Morsomme, J. Jaeken, G. Matthijs, G. De Bettignies, F. Foulquier, Glycosylation abnormalities in Gdt1p/TMEM165 deficient cells result from a defect in Golgi manganese homeostasis, Hum. Mol. Genet. 25 (2016) 1489–1500. https://doi.org/10.1093/hmg/ddw026.
[16] S. Potelle, E. Dulary, L. Climer, S. Duvet, W. Morelle, D. Vicogne, E. Lebredonchel, M. Houdou, C. Spriet, M.-A. Krzewinski-Recchi, R. Peanne, A. Klein, G. de Bettignies, P. Morsomme, G. Matthijs, T. Marquardt, V. Lupashin, F. Foulquier, Manganese-induced turnover of TMEM165, Biochem. J. 474 (2017) 1481–1493. https://doi.org/10.1042/BCJ20160910.
[17] Y. Barrandon, H. Green, Three clonal types of keratinocyte with different capacities for multiplication, Proc. Natl. Acad. Sci. U.S.A. 84 (1987) 2302–2306.
[18] S. Mukhopadhyay, C. Bachert, D.R. Smith, A.D. Linstedt, Manganese-induced trafficking and turnover of the cis-Golgi glycoprotein GPP130, Mol. Biol. Cell. 21 (2010) 1282–1292. https://doi.org/10.1091/mbc.E09-11-0985.

[19] M. Masuda, M. Braun-sommargren, D. Crooks, D.R. Smith, Golgi Phosphoprotein 4 (GPP130) is a Sensitive and Selective Cellular Target of Manganese Exposure, Synapse. 67 (2013) 205–215. https://doi.org/10.1002/syn.21632.
[20] K. Van Baelen, L. Dode, J. Vanoevelen, G. Callewaert, H. De Smedt, L. Missiaen, J.B. Parys, L. Raeymaekers, F. Wuytack, The Ca2+/Mn2+ pumps in the Golgi apparatus, Biochim. Biophys. Acta. 1742 (2004) 103–112. https://doi.org/10.1016/j.bbamcr.2004.08.018.
[21] K.M. Aberg, E. Racz, M.J. Behne, T.M. Mauro, Involucrin expression is decreased in Hailey-Hailey keratinocytes owing to increased involucrin mRNA degradation, J. Invest. Dermatol. 127 (2007) 1973–1979. https://doi.org/10.1038/sj.jid.5700785.
[22] M.J. Behne, C.-L. Tu, I. Aronchik, E. Epstein, G. Bench, D.D. Bikle, T. Pozzan, T.M. Mauro, Human keratinocyte ATP2C1 localizes to the Golgi and controls Golgi Ca2+ stores, J. Invest. Dermatol. 121 (2003) 688–694. https://doi.org/10.1046/j.1523-1747.2003.12528.x.
[23] E. Dulary, S.-Y. Yu, M. Houdou, G. de Bettignies, V. Decool, S. Potelle, S. Duvet, M.-A. Krzewinski-Recchi, A. Garat, G. Matthijs, Y. Guerardel, F. Foulquier, Investigating the function of Gdt1p in yeast Golgi glycosylation, Biochim Biophys Acta Gen Subj. 1862 (2018) 394–402. https://doi.org/10.1016/j.bbagen.2017.11.006.
[24] S. Porgpermdee, X. Yu, A. Takagi, N. Mayuzumi, H. Ogawa, S. Ikeda, Expression of SPCA1 (Hailey-Hailey disease gene product) in acantholytic dermatoses, J. Dermatol. Sci. 40 (2005) 137–140. https://doi.org/10.1016/j.jdermsci.2005.08.007.
[25] D. Muncanovic, M.H. Justesen, S.S. Preisler, P.A. Pedersen, Characterization of Hailey-Hailey Disease-mutants in presence and absence of wild type SPCA1 using Saccharomyces cerevisiae as model organism, Sci Rep. 9 (2019) 12442. https://doi.org/10.1038/s41598-019-48866-y.
[26] R.J. Fairclough, L. Dode, J. Vanoevelen, J.P. Andersen, L. Missiaen, L. Raeymaekers, F. Wuytack, A. Hovnanian, Effect of Hailey-Hailey Disease mutations on the function of a new variant of human secretory pathway Ca2+/Mn2+-ATPase (hSPCA1), J. Biol. Chem. 278 (2003) 24721–24730. https://doi.org/10.1074/jbc.M300509200.
[27] C. Dobson-Stone, R. Fairclough, E. Dunne, J. Brown, M. Dissanayake, C.S. Munro, T. Strachan, S. Burge, R. Sudbrak, A.P. Monaco, A. Hovnanian, Hailey-Hailey disease: molecular and clinical characterization of novel mutations in the ATP2C1 gene, J. Invest. Dermatol. 118 (2002) 338–343. https://doi.org/10.1046/j.0022-202x.2001.01675.x.
[28] G.E. Shull, M.L. Miller, V. Prasad, Secretory pathway stress responses as possible mechanisms of disease involving Golgi Ca2+ pump dysfunction, Biofactors. 37 (2011) 150–158. https://doi.org/10.1002/biof.141.
[29] D.D. Bikle, Z. Xie, C.-L. Tu, Calcium regulation of keratinocyte differentiation, Expert Rev Endocrinol Metab. 7 (2012) 461–472. https://doi.org/10.1586/eem.12.34.
[30] M. Houdou, E. Lebredonchel, A. Garat, S. Duvet, D. Legrand, V. Decool, A. Klein, M. Ouzzine, B. Gasnier, S Potelle, F. Foulquier, Involvement of thapsigargin– and cyclopiazonic acid–sensitive pumps in the rescue of TMEM165-associated glycosylation defects by Mn^{2+}, The FASEB Journal. 33 (2019) 2669-2679.

Figure legends

Figure 1. Expression level and subcellular localization of SPCA1 and TMEM165 in Hailey-Hailey disease patients' fibroblasts (HHD) and normal human fibroblasts as control cells (NHF). A. Total cell lysates were prepared and subjected to western-blot with SPCA1 and TMEM165 antibodies. **B.** The quantification of TMEM165 and SPCA1 expressions was done after normalization with β-actin expression using ImageJ software (number of experiments (N)=4 *: p value <0,05; ***: p value <0,005). **C.** For immunofluorescence experiments, fibroblasts were fixed and labelled with antibodies against GM130 and TMEM165 before confocal microscopy visualization. **D.** Fibroblasts were fixed and labelled with SPCA1 and TMEM165 antibodies before confocal microscopy visualization. **E.** Panels show the quantification of TMEM165 and SPCA1 associated fluorescence (N=3, number of cells n=30; *: p<0,05; **: p<0,01; ***: p<0,005; scale bar: 20µm).

Figure 2. Proximity between SPCA1 and TMEM165 proteins in HHD patients' fibroblasts and NHFs by proximity ligation assay (PLA). **A.** The PLA was performed on HHD patients' fibroblasts and NHFs with TMEM165 and SPCA1 antibodies. Each red dot represents a positive signal of protein-protein interaction and nuclei were counterstained with DAPI (blue). **B.** The PLA was performed on fibroblasts only with TMEM165 antibody or with the two antibodies on NHF 1 treated with 500µM of $MnCl_2$ for 8h which serve us as two negative controls. **C.** The quantification of the number of spots per cell observed was carried out with the ImageJ software. **D.** The quantification shows the ratio of PLA spots on SPCA1 expression levels. **E.** The PLA was performed on NHF 1 showing the colocalization of red PLA spots with Giantin-Alexa Fluor 488 which serves as Golgi marker (N=2, n=30; *: p<0,05; **: p<0,01; scale bar: 20µm, 10µm and 5µm).

Figure 3. Sensitivity of TMEM165 to $MnCl_2$ exposure in HHD patient and control fibroblasts. **A.** Cells were treated with 0 to 500µM of $MnCl_2$ for 8h. Total cell lysates were prepared and subjected to western-blot with the indicated antibodies. **B.** Panels correspond to the quantification of TMEM165 expression after normalization with β-actin expression using ImageJ software (N=3; ***: p< 0,005).

Figure 4. Impact of chloroquine treatment on the Mn^{2+} induced TMEM165 degradation in HHD patient and control fibroblasts. A. Cells were treated with 500µM (for NHFs) or 100µM (for HHD patients' fibroblasts) of $MnCl_2$ for 8h and/or 100µM of chloroquine (CQ). Total cell lysates were prepared and subjected to western-blot with the indicated antibodies. **B.** Panels show the quantification of TMEM165 expression after normalization with β-actin expression using ImageJ software (N=2; **: P<0,01; *: P<0,05).

Figure 5. Quantification of the intracellular Mn level in patient and control fibroblasts by ICP-MS followed $MnCl_2$ supplementation. A. Cells were treated or not with 5µM of $MnCl_2$ for 1h and 2h. Panel shows the quantification of the total cellular Mn level in HHD patients' fibroblasts and control fibroblasts after normalization with the protein concentration. **B.** Panel indicates the average of the quantification of the total cellular Mn level in all HHD fibroblasts compared to control fibroblasts (N=1).

Figure 6. Average of the quantification of GPP130 fluorescence intensity under $MnCl_2$ exposure in HHD fibroblasts versus control fibroblasts. Panel shows the mean GPP130 fluorescence intensity in HHD fibroblasts compared to control fibroblasts treated or not with 500µM MnCl2 for 0, 8h, 12h and 24h (N=1, n=30).

Figure 7. Sensitivity of TMEM165 to $MnCl_2$ exposure in HHD patient and control keratinocytes, differentiated or not. Undifferentiated keratinocytes (**A**) and differentiated keratinocytes (**B**) were treated with 50µM of $MnCl_2$ for 48h. Keratinocytes were differentiated by adding 1.2mM $CaCl_2$ in the cell culture medium for 7 days. Total cell lysates were prepared and subjected to western-blot with the indicated antibodies. Right panels show the quantification of TMEM165 expression after normalization with β-tubulin expression using ImageJ software. **C**. Panels indicate the average of the quantification of TMEM165 expression in all HHD keratinocytes compared to control keratinocytes (N=1).

Figure S1 Expression level and subcellular localization of SPCA1 and TMEM165 in HHD and control fibroblasts followed increasing $MnCl_2$ concentrations. A. Cells were treated with 0 to 500µM $MnCl_2$ for 8h, fixed and labeled with antibodies against TMEM165 and SPCA1 before confocal microscopy visualization. DAPI staining shows the nucleus. Right panels show the quantification of TMEM165 associated fluorescence intensity. **B.** Panel

shows the quantification of the mean intensity of TMEM165 associated fluorescence in all fibroblasts (N=2; number of cells n=30; scale bar: 20µm; ***: p<0,005).

Figure S2. Determination of the relative EC50 of $MnCl_2$ concentration for each HHD and control fibroblasts. Cells were treated with 0, 1, 10, 50, 100 and 300µM $MnCl_2$ for 8h, fixed and labeled with antibodies against TMEM165 before confocal microscopy visualization. The quantification of TMEM165 associated fluorescence intensity was performed as described elsewhere for each $MnCl_2$ concentration and the determination of the EC50 was done using the software *https://www.aatbio.com/tools/ec50-calculator* (N=1)

Figure S3. Impact of chloroquine treatment on the Mn^{2+} induced TMEM165 degradation in HHD patient and control fibroblasts. Cells were treated with 500µM (for NHFs) or 100µM (for HHD patients' fibroblasts) of $MnCl_2$ and/or 100µM of CQ for 8h. Cells were fixed and labeled with antibodies against TMEM165 (upper panels) and LAMP2 (middle panels), a lysosomal marker, before confocal microscopy visualization. DAPI staining shows the nucleus. Right panels show the quantification of TMEM165 associated fluorescence intensity (N=2, n=30; scale bar: 20µm and 10µm for zoom).

Figure S4. Expression level of TMEM165 in HHD and control fibroblasts in presence of 5µM of $MnCl_2$. Cells were treated with 5µM $MnCl_2$ for 1h and 2h. Total cell lysates were prepared and subjected to western-blot with TMEM165 antibody. Bottom panel indicates the quantification of TMEM165 expression after normalization with β-actin expression using ImageJ software (N=1).

Figure S5. Sensitivity of GPP130, a Golgi manganese sensor, to $MnCl_2$ exposure in HHD patient and control fibroblasts. Cells were treated with 500µM $MnCl_2$ for 0, 8h, 12h and 24h, and fixed then labeled with antibodies against GPP130 (right panel), a Golgi Mn2+ sensor and marker, before confocal microscopy visualization. Left panel show the quantification of GPP130 associated fluorescence intensity in control fibroblasts compared to HHD fibroblasts. (N=1; n=30; scale bar: 20µM).

Table 1. ***ATP2C1*** **mutations from HHD patient fibroblasts (A) and keratinocytes (B) used in this study**

A.

Patients	cDNA change[a]	Protein change[b]	Location	Protein domain	References
HHD 1	c.2126+2dup	/	Intron 22	M5	/

HHD 2*	c.1738A>G	p.Ile580Val	Exon 18	ATP binding	[4], [23], [25]
HHD 3	c.1738A>G	p.Ile580Val	Exon 18	ATP binding	[4], [23], [25]
HHD 4	c.484_496del	p.Cys162Glyfs*23	Exon 7	A	/

B.

Patients	**cDNA change[a]**	**Protein change[b]**	**Location**	**Protein domain**	**References**
HHD 2*	c.1738A>G	p.Ile580Val	Exon 18	ATP binding	[4], [25]
HHD 5	c.1076T>A	p.Met359Lys	Exon 13	M5	/
HHD 6	c.2375delTTGT	p.Phe792Serfs*10	Exon 24	M7	[4]

[a] Nucleotides are numbered according to *ATP2C1* cDNA sequence, with the first nucleotide of ATG initiation codon as 1.

[b] Amino acids are numbered according to the predicted ATP2C1 peptide sequence.

* Keratinocytes and fibroblasts of the same HHD patient

A.

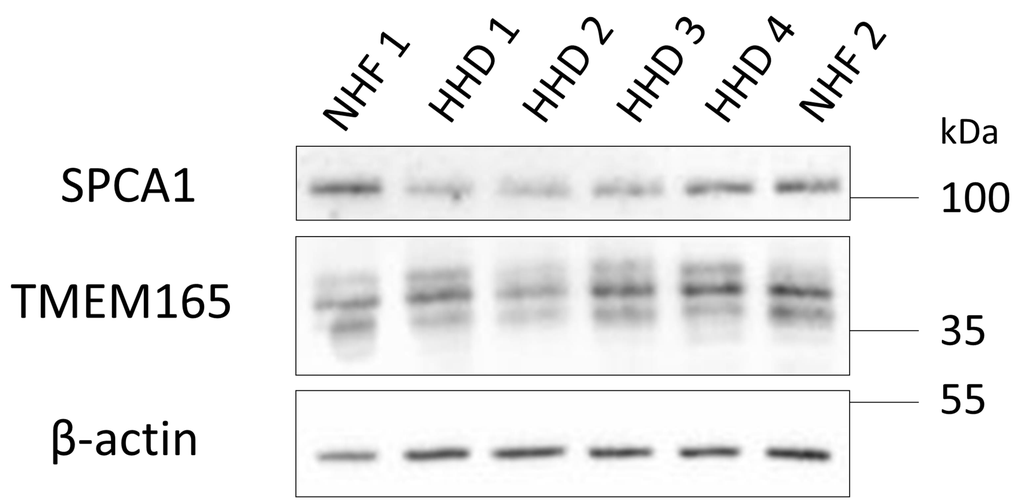

B.

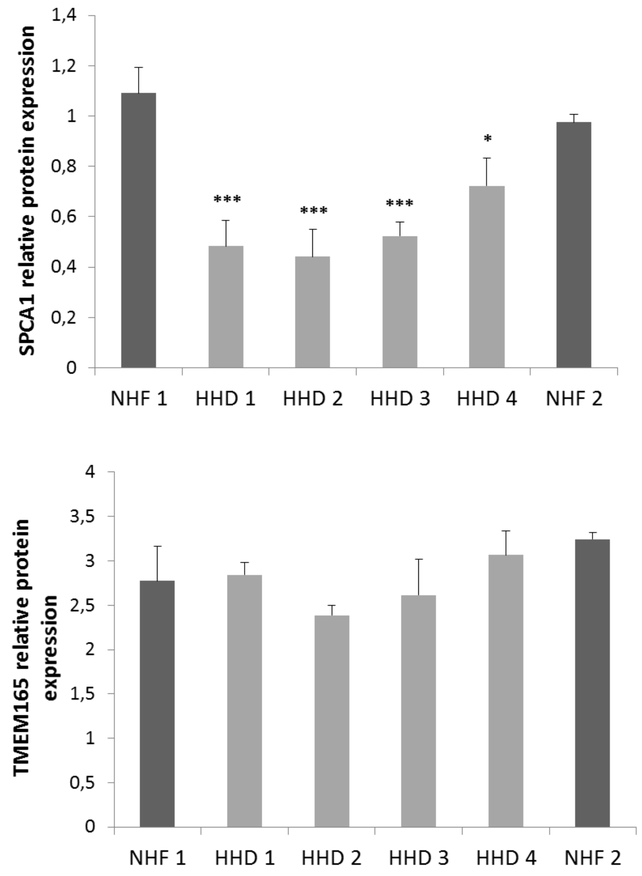

C.

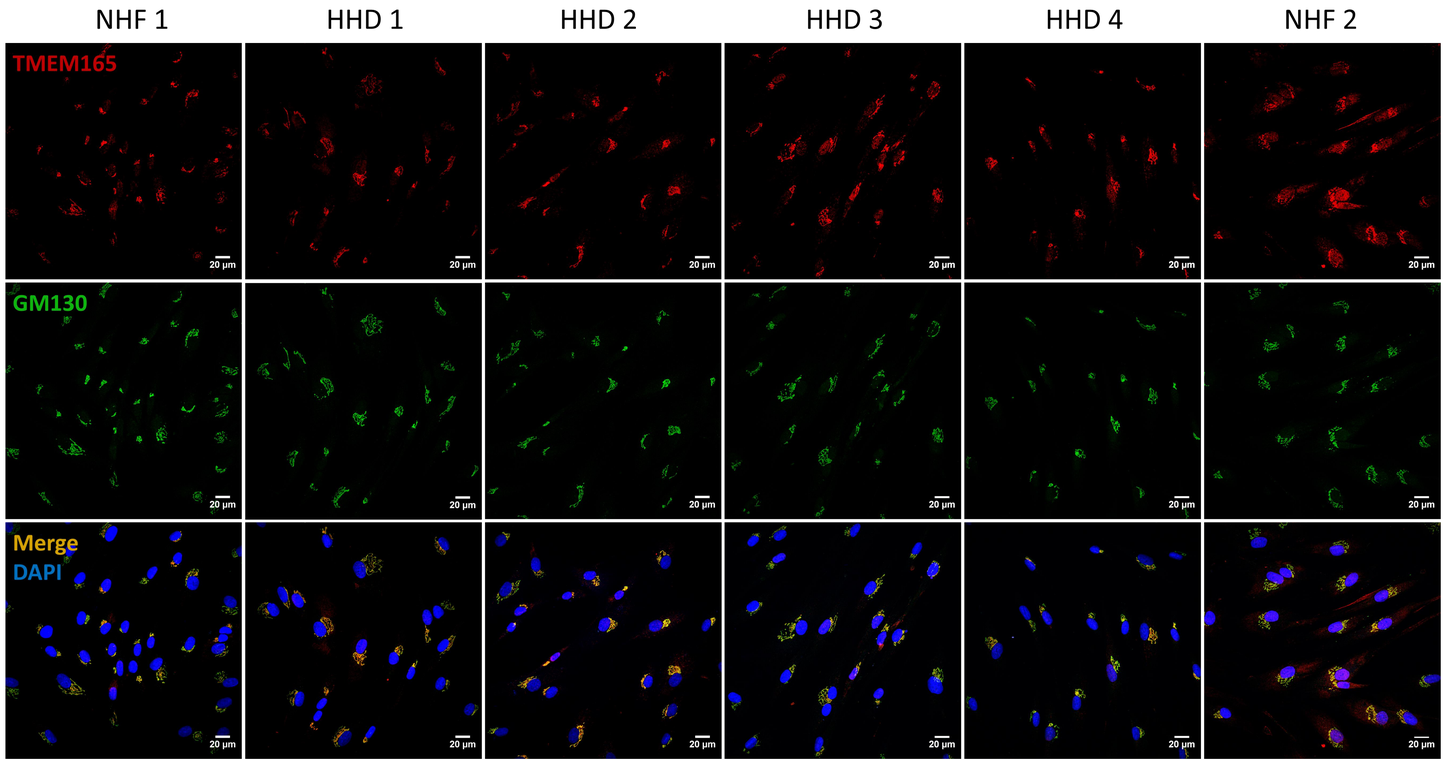

D.

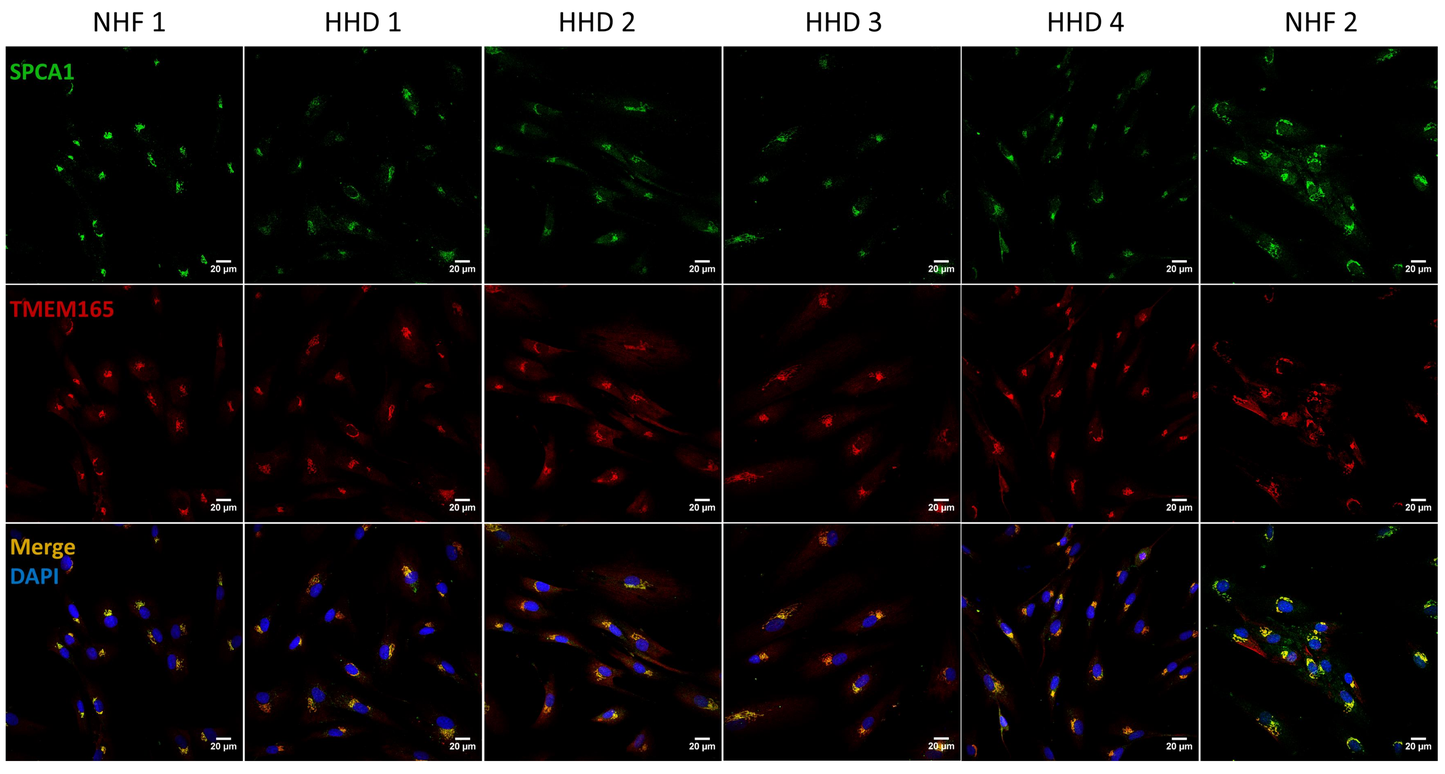

E.

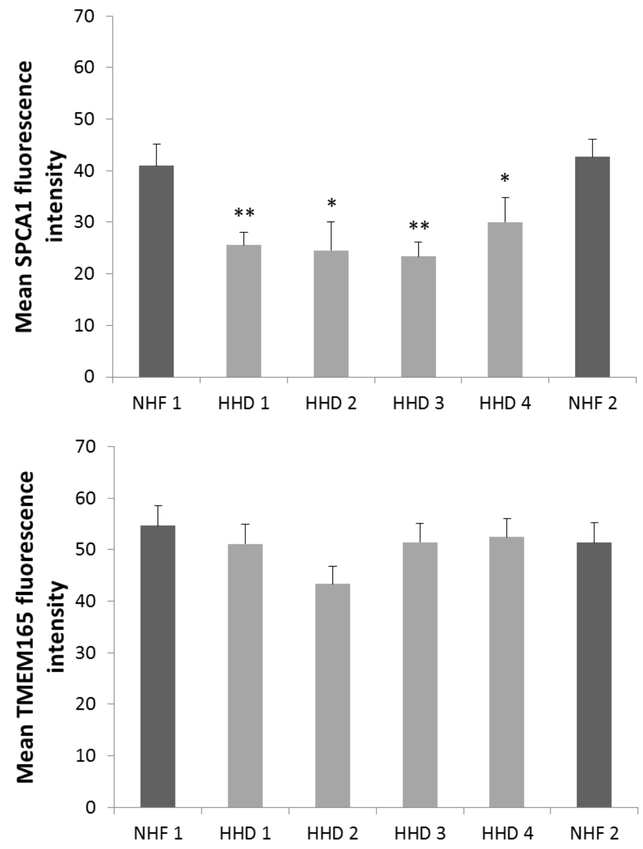

Figure 1

Figure 2

A.

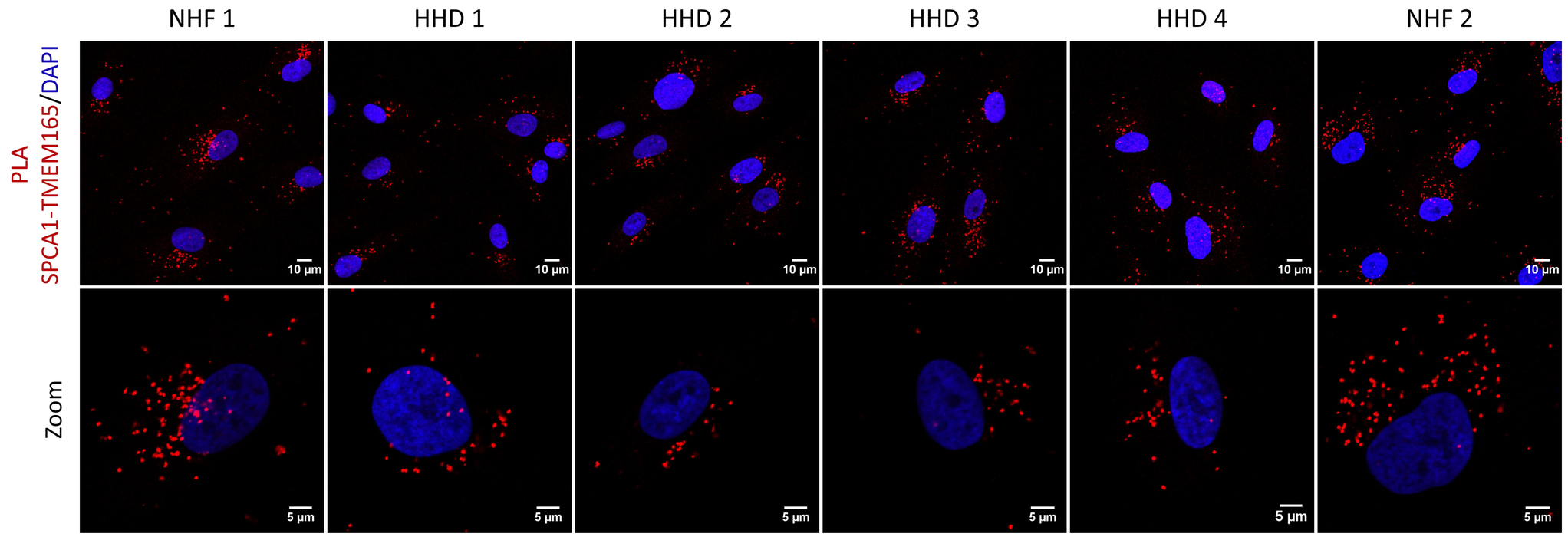

B.

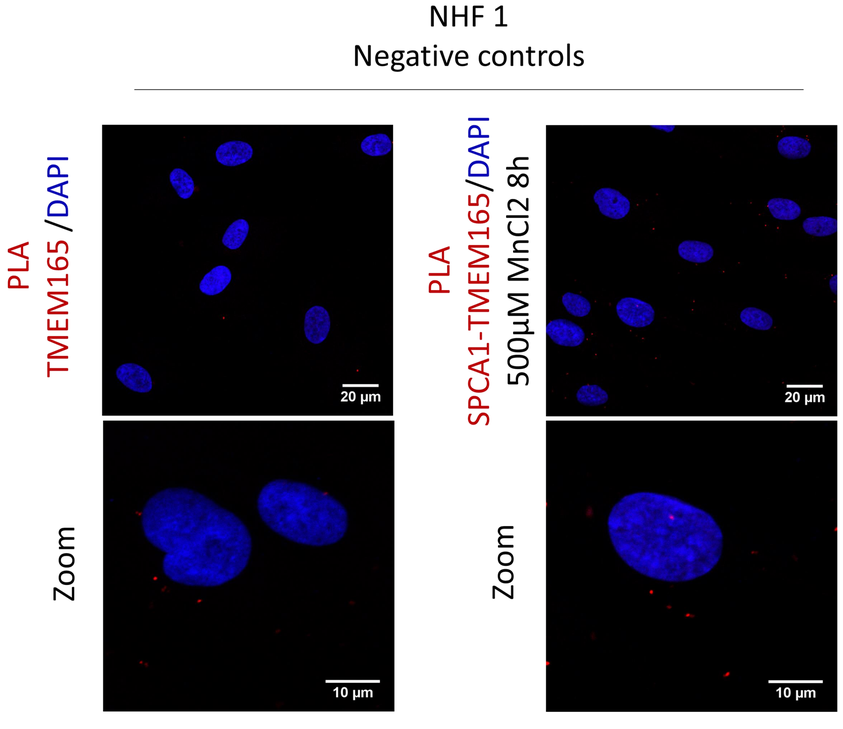

C.

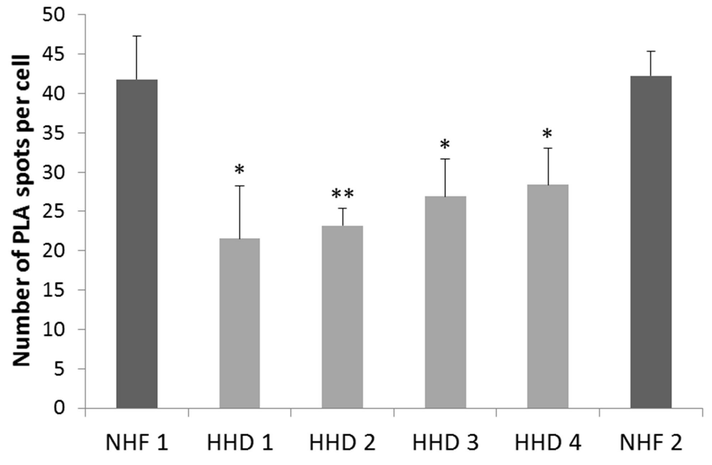

D.

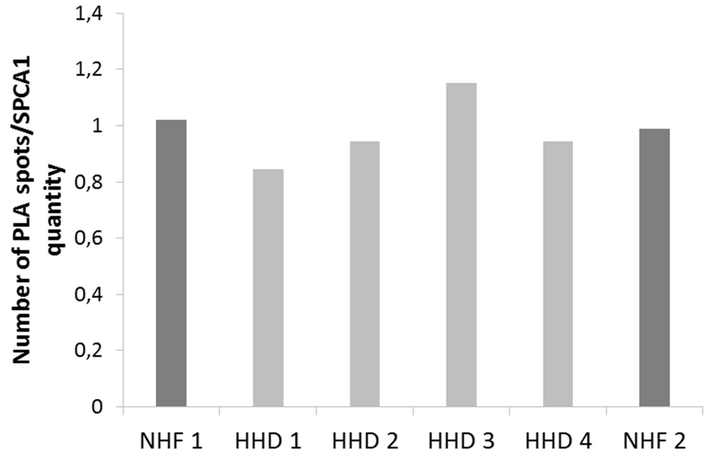

E.

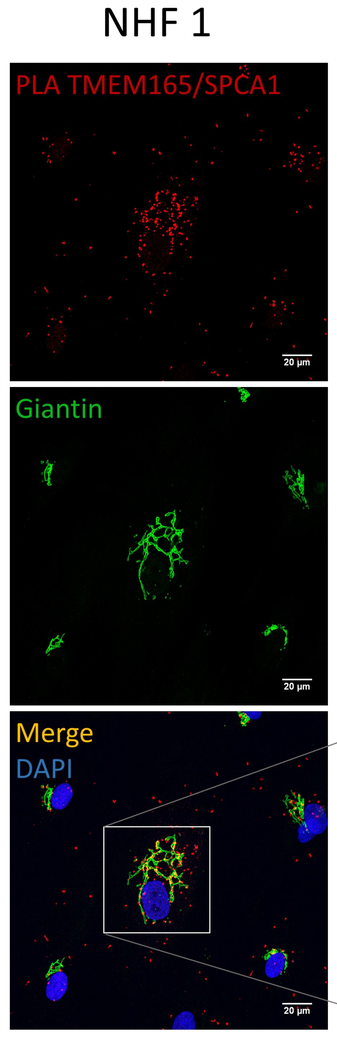

Figure 3

A.

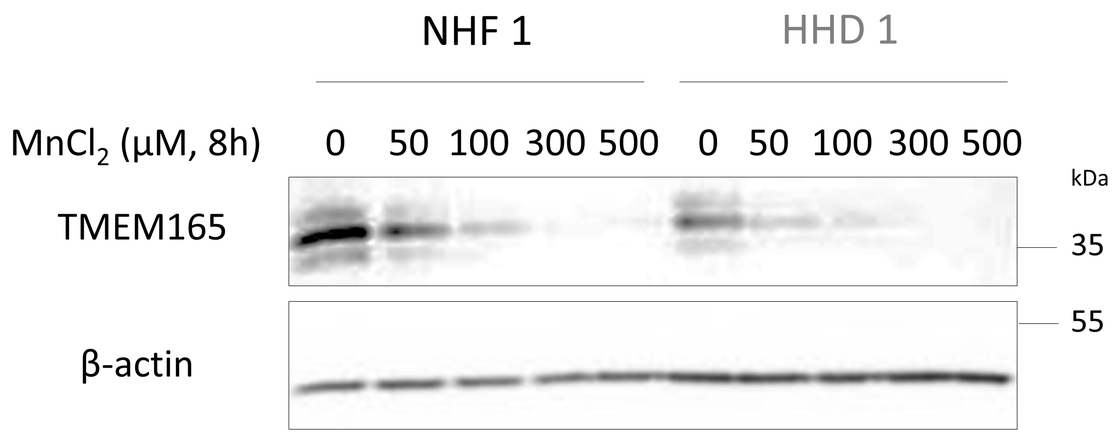
NHF 1
HHD 1
MnCl2 (µM, 8h)
0 50 100 300 500 0 50 100 300 500
kDa
TMEM165
35
β-actin
55

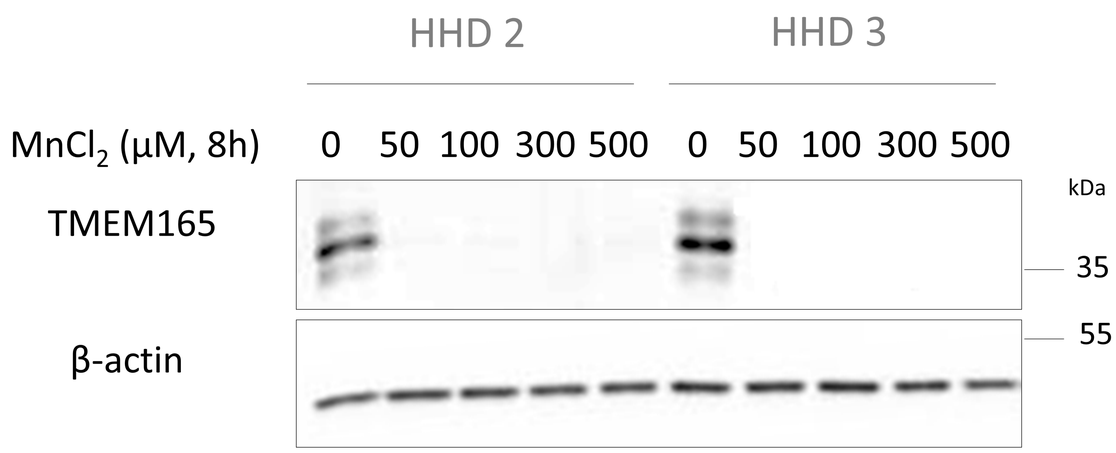
HHD 2
HHD 3
MnCl2 (µM, 8h)
0 50 100 300 500 0 50 100 300 500
kDa
TMEM165
35
β-actin
55

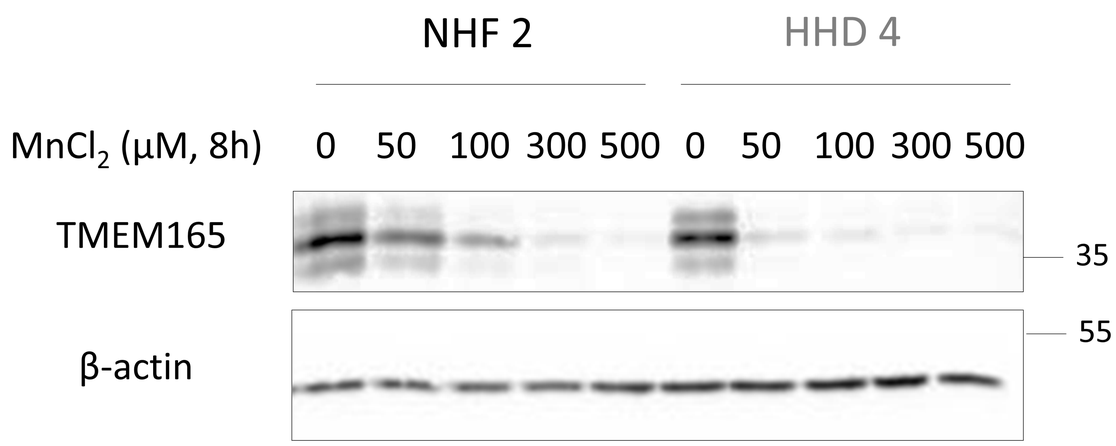
NHF 2
HHD 4
MnCl2 (µM, 8h)
0 50 100 300 500 0 50 100 300 500
TMEM165
35
β-actin
55

B.

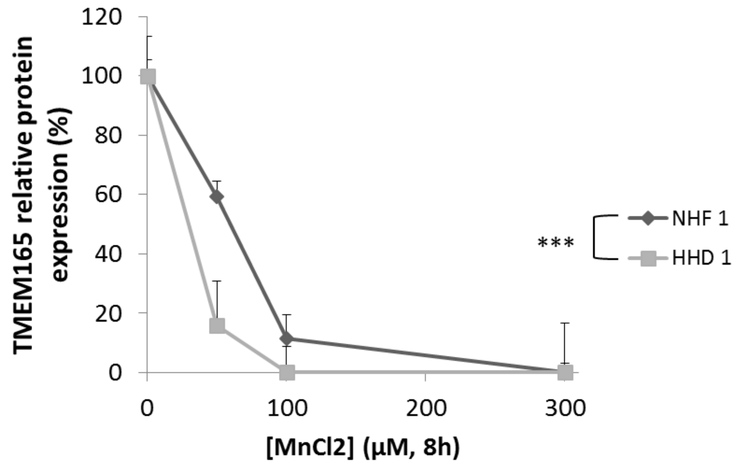
TMEM165 relative protein expression (%)
120
100
80
60
40
20
0
0
100
200
300
[MnCl2] (µM, 8h)
***
NHF 1
HHD 1

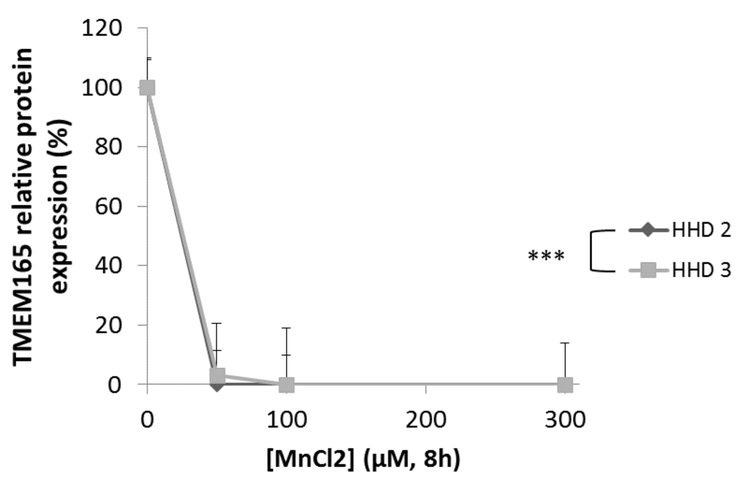
TMEM165 relative protein expression (%)
120
100
80
60
40
20
0
0
100
200
300
[MnCl2] (µM, 8h)
***
HHD 2
HHD 3

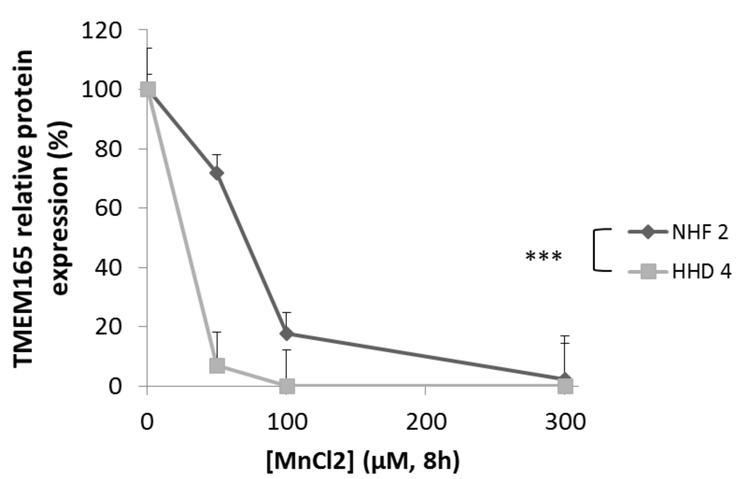
TMEM165 relative protein expression (%)
120
100
80
60
40
20
0
0
100
200
300
[MnCl2] (µM, 8h)
***
NHF 2
HHD 4

Figure 4

A.

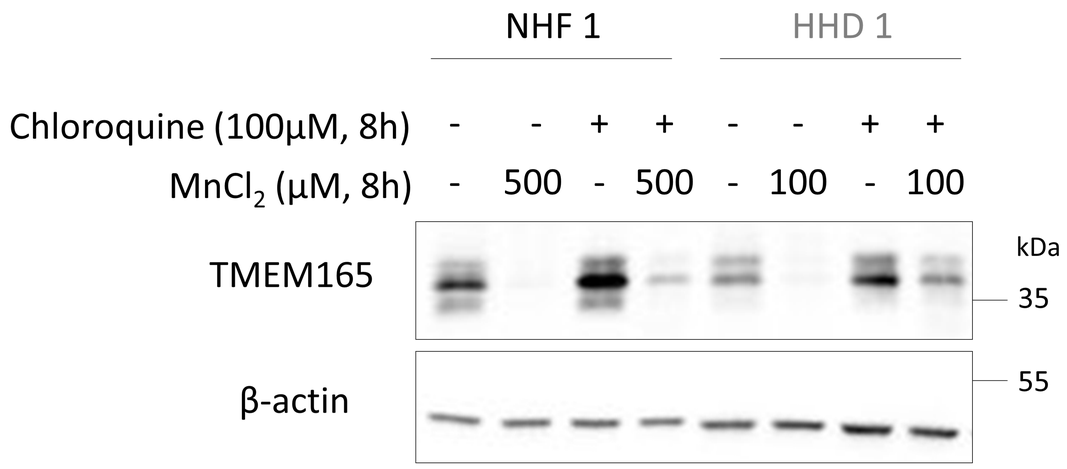
NHF 1
HHD 1
Chloroquine (100µM, 8h) - - + + - - + +
MnCl2 (µM, 8h) - 500 - 500 - 100 - 100
TMEM165
β-actin
kDa
35
55

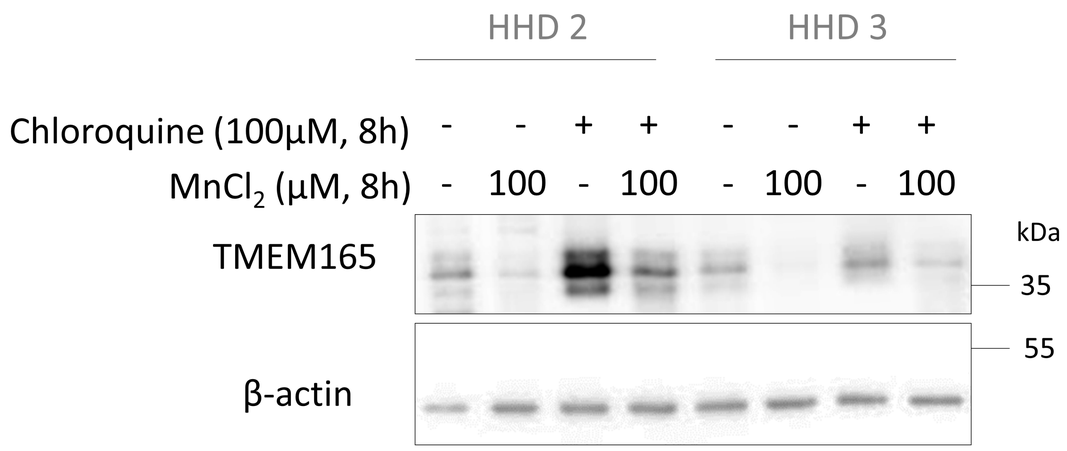
HHD 2
HHD 3
Chloroquine (100µM, 8h) - - + + - - + +
MnCl2 (µM, 8h) - 100 - 100 - 100 - 100
TMEM165
β-actin
kDa
35
55

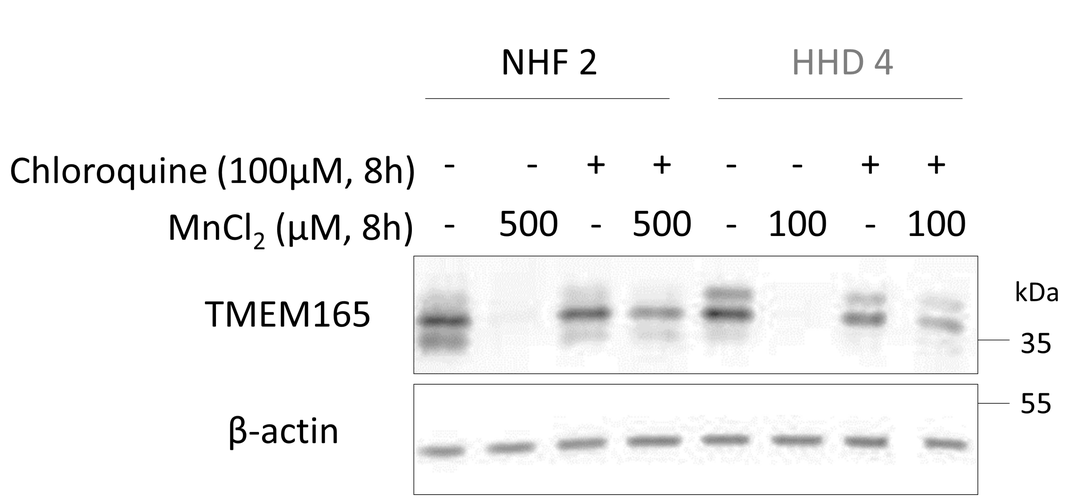
NHF 2
HHD 4
Chloroquine (100µM, 8h) - - + + - - + +
MnCl2 (µM, 8h) - 500 - 500 - 100 - 100
TMEM165
β-actin
kDa
35
55

B.

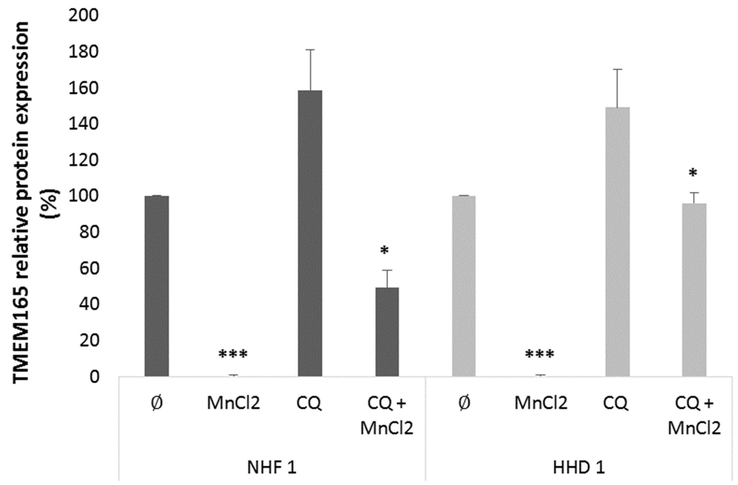
TMEM165 relative protein expression (%)
200
180
160
140
120
100
80
60
40
20
0
***
*
Ø
MnCl2
CQ
CQ + MnCl2
NHF 1
HHD 1

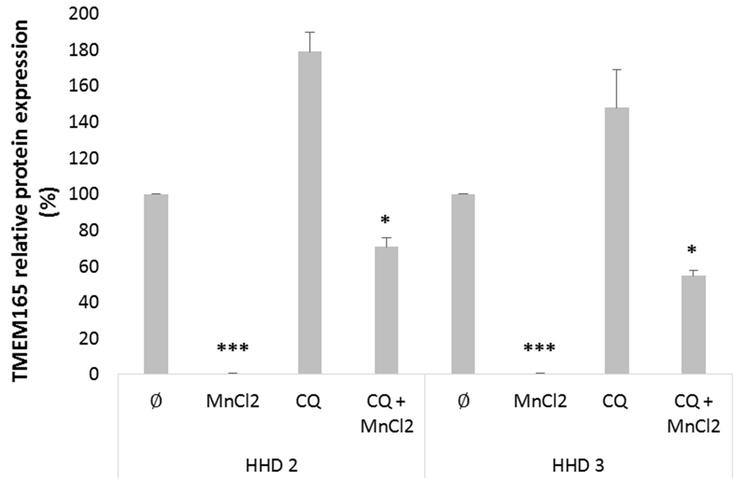
TMEM165 relative protein expression (%)
200
180
160
140
120
100
80
60
40
20
0
***
*
Ø
MnCl2
CQ
CQ + MnCl2
HHD 2
HHD 3

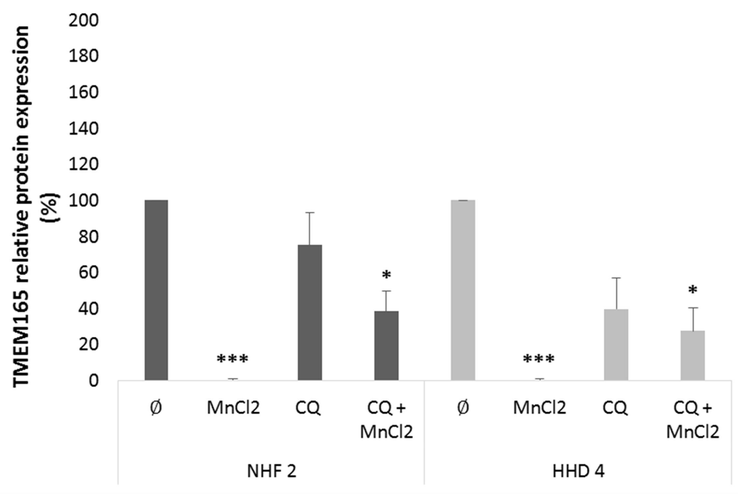
TMEM165 relative protein expression (%)
200
180
160
140
120
100
80
60
40
20
0
***
*
Ø
MnCl2
CQ
CQ + MnCl2
NHF 2
HHD 4

Figure 5

A.

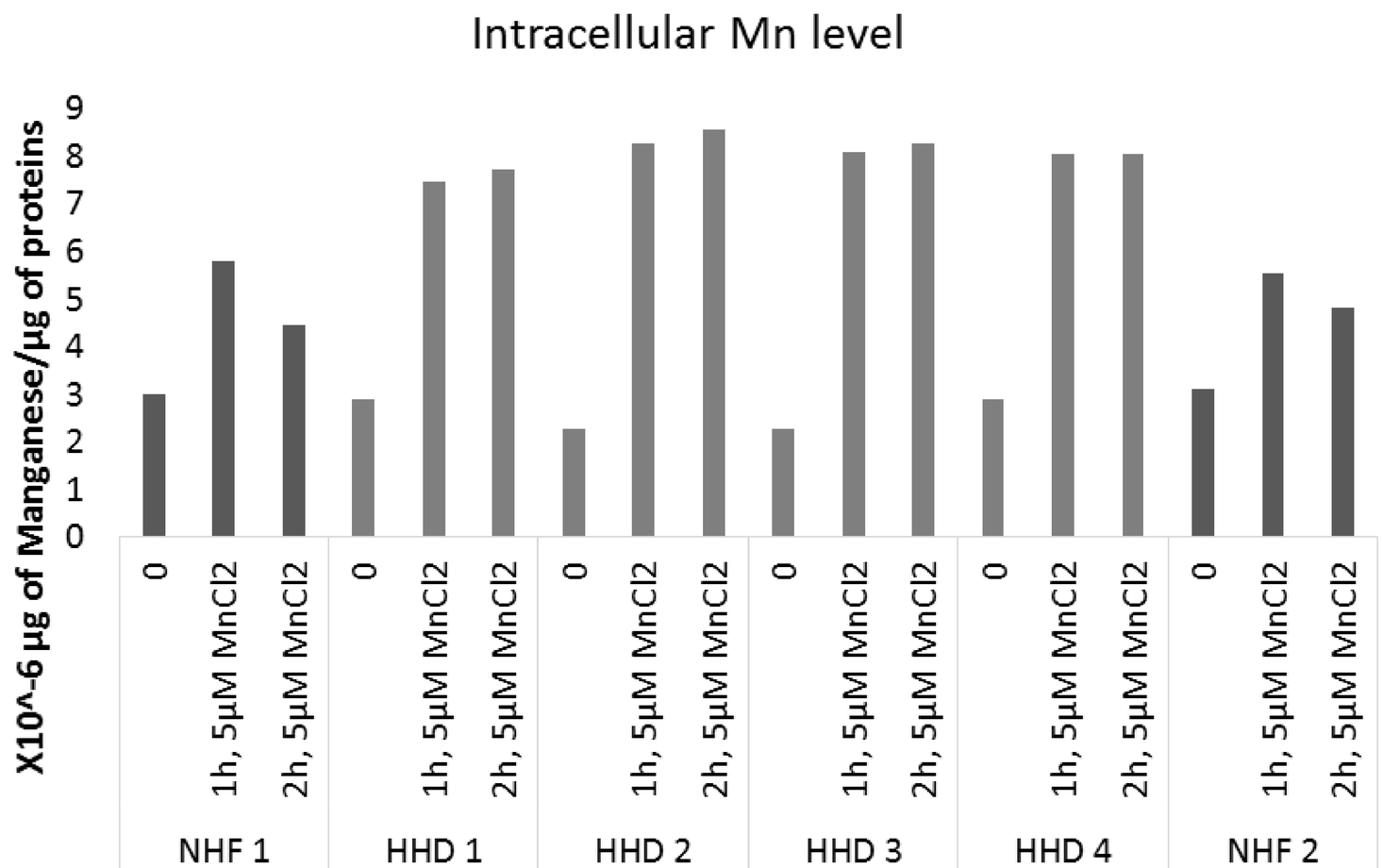
Intracellular Mn level
X10^-6 µg of Manganese/µg of proteins
0
1
2
3
4
5
6
7
8
9
0
1h, 5µM MnCl2
2h, 5µM MnCl2
NHF 1
HHD 1
HHD 2
HHD 3
HHD 4
NHF 2

B.

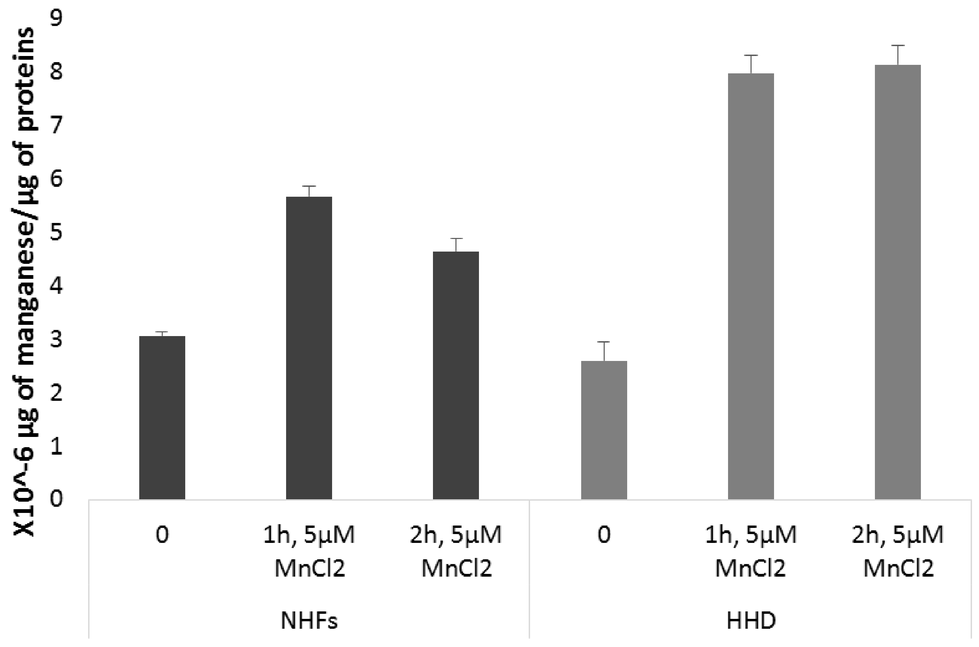
X10^-6 µg of manganese/µg of proteins
0
1
2
3
4
5
6
7
8
9
0
1h, 5µM MnCl2
2h, 5µM MnCl2
NHFs
HHD

Figure 6

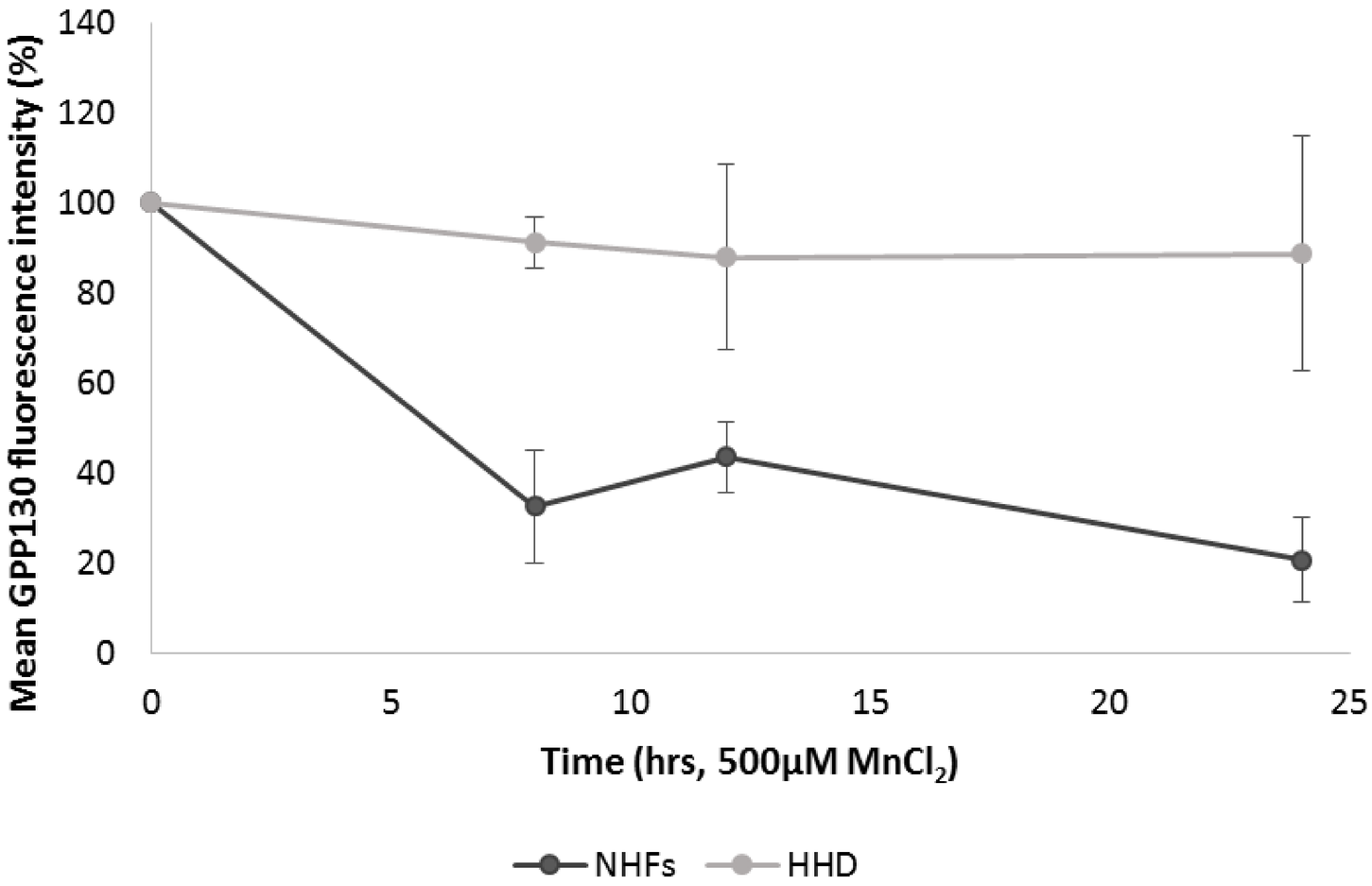
Mean GPP130 fluorescence intensity (%)
140
120
100
80
60
40
20
0
0
5
10
15
20
25
Time (hrs, 500µM MnCl2)
NHFs
HHD

Figure 7

A.

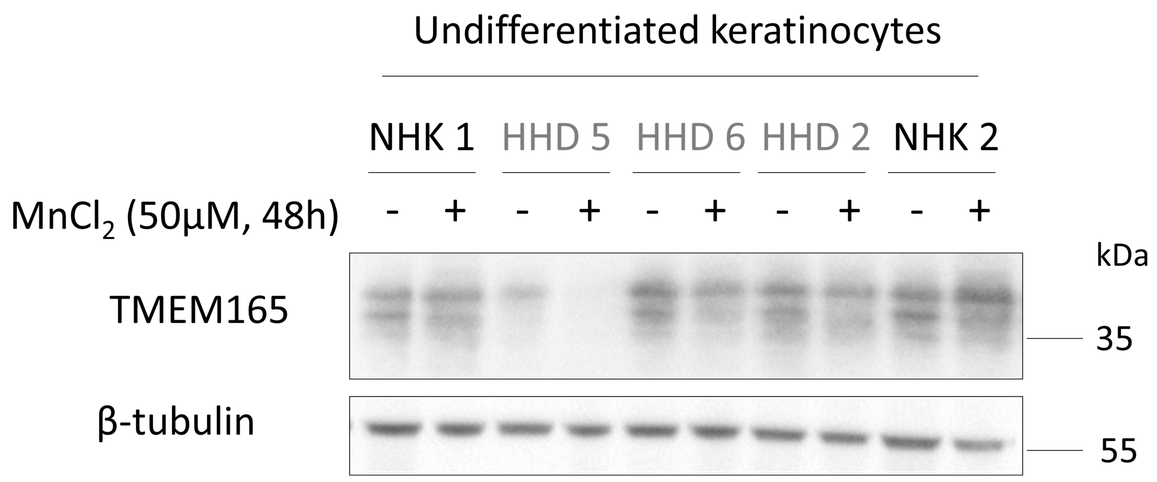
Undifferentiated keratinocytes
NHK 1
HHD 5
HHD 6
HHD 2
NHK 2
MnCl2 (50µM, 48h)
- + - + - + - + - +
kDa
TMEM165
35
β-tubulin
55

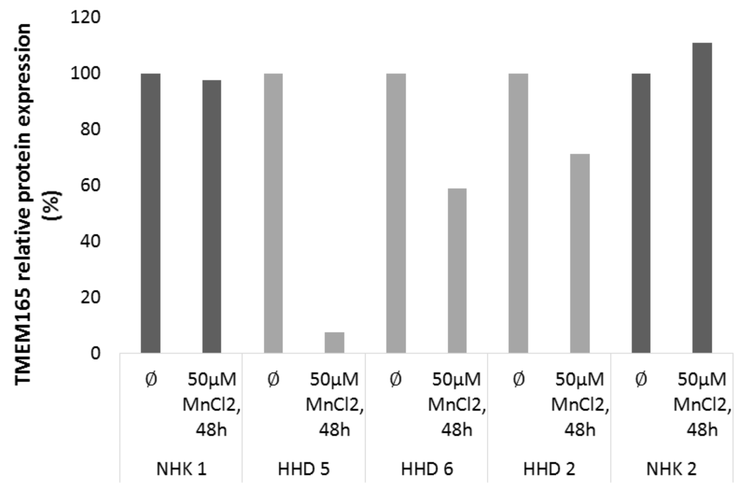
TMEM165 relative protein expression (%)
120
100
80
60
40
20
0
Ø
50µM MnCl2, 48h
NHK 1
HHD 5
HHD 6
HHD 2
NHK 2

B.

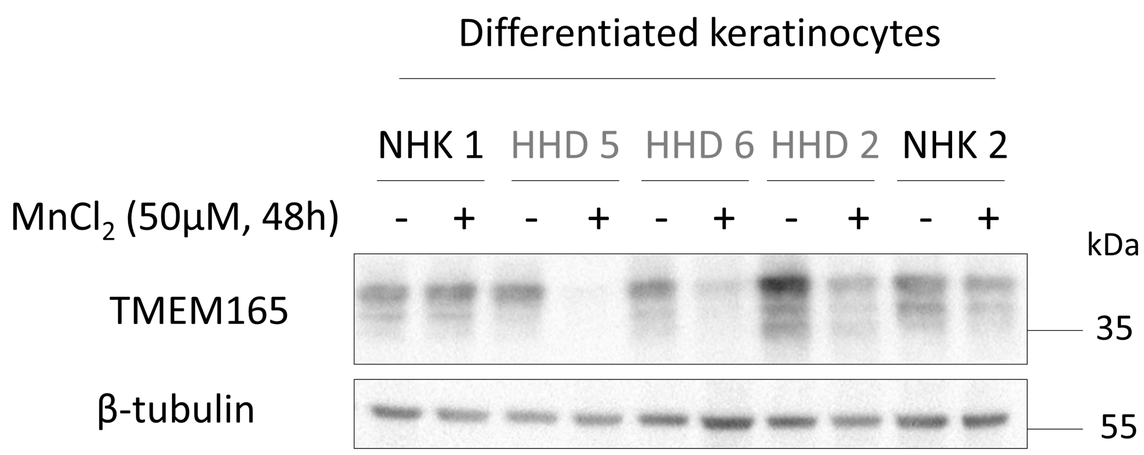
Differentiated keratinocytes
NHK 1
HHD 5
HHD 6
HHD 2
NHK 2
MnCl2 (50µM, 48h)
- + - + - + - + - +
kDa
TMEM165
35
β-tubulin
55

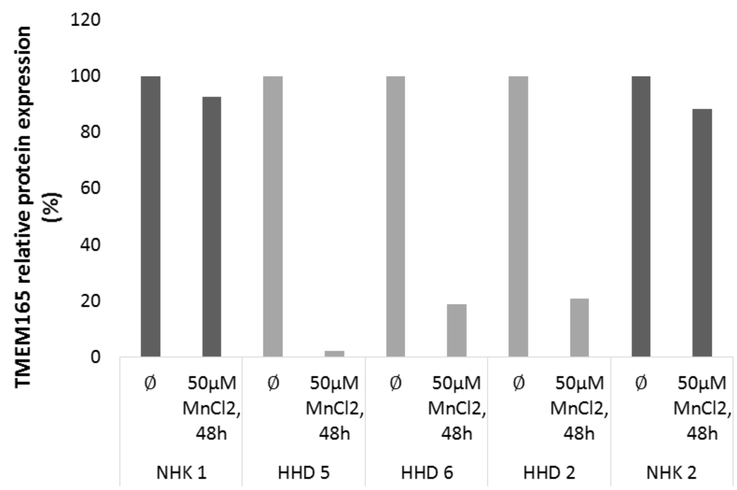
TMEM165 relative protein expression (%)
120
100
80
60
40
20
0
Ø
50µM MnCl2, 48h
NHK 1
HHD 5
HHD 6
HHD 2
NHK 2

C.

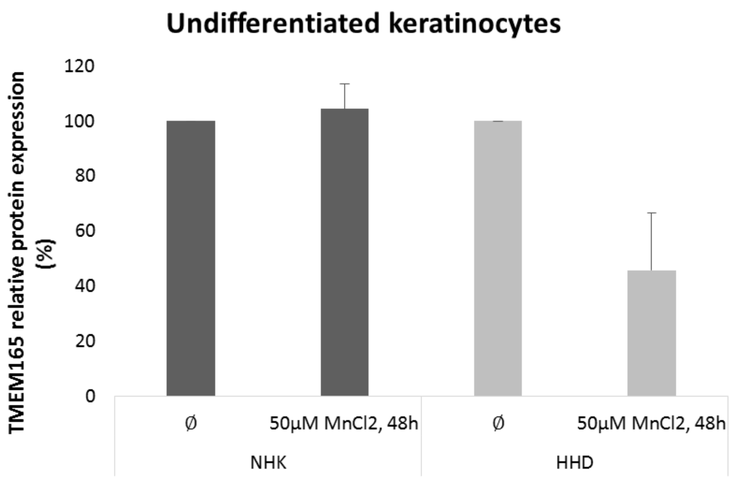
Undifferentiated keratinocytes
TMEM165 relative protein expression (%)
120
100
80
60
40
20
0
Ø
50µM MnCl2, 48h
NHK
HHD

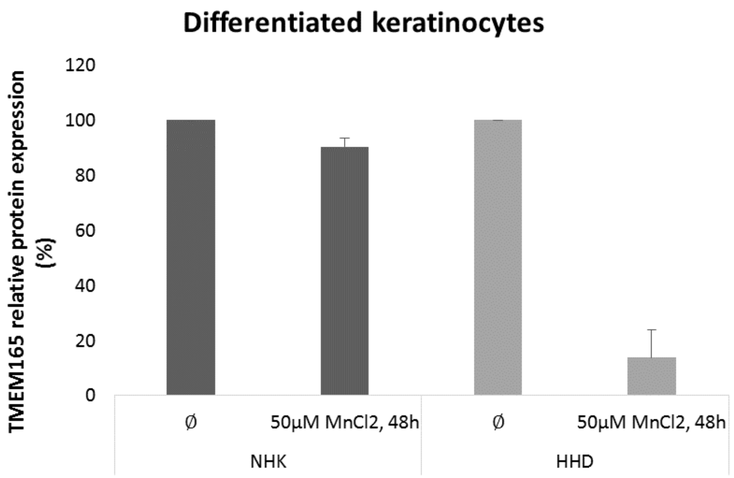
Differentiated keratinocytes
TMEM165 relative protein expression (%)
120
100
80
60
40
20
0
Ø
50µM MnCl2, 48h
NHK
HHD